CSUFlow25: Colorado Streamflow Ungaged Prediction Models

Kathryn Willi[1], Stephanie Kampf[1], William Keenan[1], Juan De La Torre[1], Matthew R.V. Ross[1]

[1] Colorado State University, Fort Collins, Colorado, USA

Corresponding author: Stephanie Kampf, stephanie.kampf@colostate.edu

Corresponding author ORCID: 0000-0001-8991-2679

Abstract

CSUFlow25 is an updated set of statistical models for predicting streamflow in ungaged basins in Colorado, USA. It builds on the earlier CSUFlow18 models (Eurich et al., 2021) by extending the streamflow record from water years 2001–2018 to 2001–2024, expanding the pool of candidate predictor variables, and increasing the number of streamflow metrics predicted. Models were developed from a rigorously screened dataset of 131 watersheds in Colorado and surrounding states, with sites filtered for transbasin diversions, large dams at watershed outlets, urban land use, and nested watersheds to better represent natural streamflow. Multiple linear regression models were fit for mean annual and mean monthly flows, high and low flows (Qmax, Q95, Qmin, Q5), the date of those flow quantiles, the fraction of annual flow during the monsoon season, and bankfull (1.5-year return period) flow, using predictors describing topography, climate, geology, land cover, soil, and hydrologic region. Model generalizability was assessed with 5-fold cross-validation and evaluated using the Nash–Sutcliffe efficiency (NSE) and percent bias (PBIAS). Performance is strongest for mean annual flow, snowmelt-season monthly flows, high flows, and bankfull flow, and weaker for low flows, winter months, and the monsoon fraction. Across nearly all months CSUFlow25 outperforms both CSUFlow18 and the development version of USGS StreamStats. The models are implemented in a publicly available R Shiny application that delineates a watershed from a user-selected point, compiles predictor variables, and returns predicted flow values with 95% confidence intervals.

Keywords: ungaged basins; streamflow prediction; regional regression; Colorado; hydrology

Data and code availability: The CSUFlow25 models are available as an interactive application at https://geocentroid.shinyapps.io/CSUFlow25/. Code used to generate the models is available at https://github.com/rossyndicate/CSUFlow25_Workflow.

Conflict of interest: The authors declare no conflicts of interest.

Table of Contents

1. Introduction

This report describes the updated version of CSUFlow18, an ungaged streamflow prediction model for Colorado (Eurich et al. 2021). The original CSUFlow18 predicted mean annual and mean monthly flows and was developed using streamflow data from 2001-2018. Predictor variables included topography, geology, climate, and hydrologic region variables. The updated models use a longer time period of data (2001-2024), expand the number of potential predictor variables, and expand the number of streamflow variables predicted. The following sections describe the model training dataset, model development and testing, and model implementation.

2. Dataset

The CSUFlow25 models are developed using streamflow data from stream gaging sites in Colorado and surrounding states. Following some of Eurich et al., (2021), we selected gaging sites with the following rules: the drainage areas for the sites must be ≤1,500 km^2; have >85% data availability for at least 20 years between water years 2000-2024, and be within 200 miles of the Colorado border. The data completeness criteria are stricter than those of Eurich et al. (2021) to ensure that values included in model development are as accurate as possible. Gaps in discharge data of seven days or fewer were filled in with linear interpolation.

Another difference from Eurich et al. (2021) is that we included gages outside of Colorado. Colorado alone has few stream gages in the Plains and Northwest regions, so adding gages from surrounding states helps us gain information for streamflow conditions near these poorly monitored regions. This addition of gages is supported by prior research in which we found that annual streamflow relationships to precipitation and snow are similar between Colorado and surrounding states (Hammond et al., 2018). Additional research also highlights that ungaged basin discharge can be consistently predicted by nearby gages (Vlah et al., 2024), highlighting the need to comprehensively search for gages near Colorado even if they are not in the state.

Next, we screened watersheds for transbasin diversions, flow modifications, and urban land use. All watersheds with known transbasin diversions were excluded from the dataset. Transbasin diversions were identified with several automated and manual procedures including: identifying National Hydrography Dataset (NHD) flowlines that crossed the watershed boundary, remarks that describe transbasin diversions on the USGS NWIS site, or transbasin diversion points in a shapefile provided by Colorado Water Conservation Board (CWCB). For flow modifications, we reviewed the classifications of flow lines in NHD; the dam storage values in StreamCat, a dataset compiled by the US Environmental Protection Agency (Hill et al. 2016), and the remarks for each USGS site, which are available from the water year summary information. Sites with some flow modifications needed to be included to have a large enough dataset, so we kept most of the watersheds where the flow modifications were contained within the watershed boundaries, consistent with Eurich et al. (2021). However, in contrast to Eurich et al. (2021), we excluded sites with dams at the watershed outlet directly above the stream gage, as these can control the flow of the entire gaged stream. To screen for urban area, we used the percent of drainage area classified as developed in StreamCat (Hill et al. 2016) and excluded watersheds with >10% urban area.

Finally, we reviewed the remaining watersheds to see if they were nested. In cases with nested watersheds, we used only the upstream watershed to avoid double-counting flow conditions in model development. Exceptions to this rule are downstream sites that capture additional large tributaries that are not measured by the upstream sites. This overall process of reviewing watersheds was more rigorous than for Eurich et al. (2021), so some of the watersheds that had been used to develop CSUFlow18 are not used in CSUFlow25 development. The watersheds we used for model development are shown in Figure 1 and listed in Table A1, and the watersheds excluded are shown in Figure 1 and Table A2. The complete dataset now includes 131 watersheds.

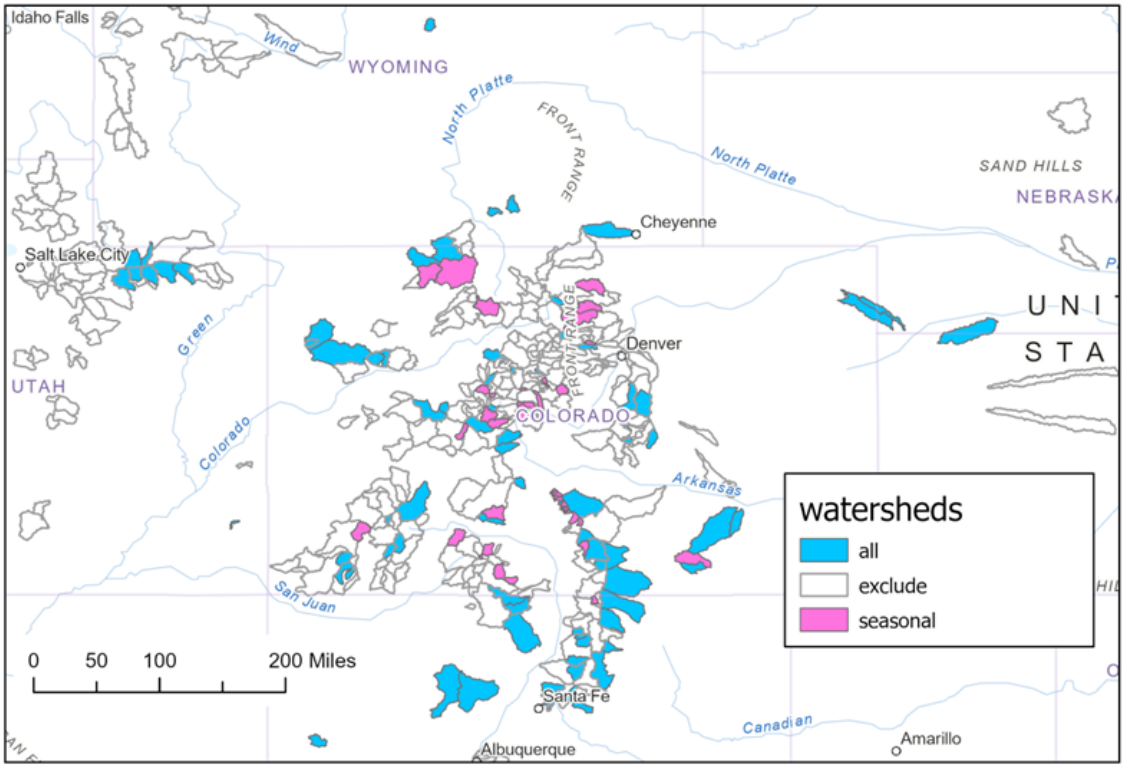

Figure 1. Watersheds considered for developing CSUFlow25. "All" indicates watersheds used in model development for all flow variables; "seasonal" indicates watersheds that only had complete data for part of the year. "Exclude" indicates watersheds that were excluded due to transbasin diversions, large dams at the watershed outlets, distance >200 miles from Colorado border, >10% urban area, or downstream from another watershed already included in the dataset.

For each site included in the dataset (Table A1), we computed mean annual and mean monthly flow, metrics representing low flows and high flows, dates of flow quantiles, fraction of annual flow during the monsoon season, and bankfull flow. The variable names and descriptions are given in Table 1. All flow values in the modeling are normalized by drainage area and provided in mm or mm/d.

For low and high flows we included the mean of annual minimum daily flows and mean of annual maximum daily flows. We also computed flow duration curves for each site and extracted the 5th percentile values (Q5) to represent low flows and 95th percentile values (Q95) to represent high flows. For flow timing, we used quantiles of cumulative water year flow in increments of 10%. These represent

the average day of water year when each percentage of water year total flow has passed the stream gage (Day10-Day90). To represent the influence of the monsoon on streamflow, we computed the fraction of total water year flow that happens during the monsoon months (July-September).

Table 1. Streamflow variables included in CSUFlow25.

Variable ID	Name	Type	Units
Qann	Mean annual (water year) total flow	Average conditions	mm
Qjan - Qdec	Mean monthly total flow	Average conditions	mm
Qmin	Mean annual minimum flow	Low flow	mm/d
Q5	5th percentile of daily streamflow	Low flow	mm/d
Qmax	Mean annual maximum daily flow	High flow	mm/d
Q95	95th percentile of daily streamflow	High flow	mm/d
Day10 - Day90	Flow quantiles: Day of water year when 10% (up to 90% in increments of 10) of the total flow has passed the gage	Flow timing	Day of water year
Monsoon	Fraction of total water year flow that comes during July-Sep	Flow timing	fraction
Bankfull	1.5 year return period flow rate	Flow timing	mm/d

Finally, to estimate bankfull flow we used the 1.5 return period flow value, which is a standard choice for bankfull estimation (Simon et al., 2004). We also compiled information from prior research to evaluate whether this 1.5 return period flow is a suitable representation of bankfull for Colorado streams. To do this we computed the return periods of literature-documented bankfull flow values. The 1.5 year return period represents the bankfull flow condition well at three of the streams for which we found bankfull flow rates in prior literature (Michigan River, Middle Boulder Creek, and Black Gore Creek). For other streams in Colorado, the bankfull flow has a longer return period, up to 5.4 years (Table 2). Another study

on streams in Idaho found return periods of bankfull flow ranging from 1.1-4.8 years (Whiting et al., 1999), similar to the range in Colorado.

Table 2. Return periods of bankfull flow based on prior measurements at Colorado Streams

Site	Bankfull flow (cfs)	Return period (yr)
Michigan River Near Cameron Pass, CO	25[1]	1.57
Halfmoon Creek Near Malta, CO	250 [1]	4.75
Chalk Creek at Nathrop	345[1]	3.06
Crystal River Abv Avalanche Crk, Near Redstone, CO	1730[1]	1.79
Little Snake River Near Slater, CO	2549[1]	5.4
Lake Fork at Gateview, CO	1483[1]	2.74
Middle Boulder Creek at Nederland, CO	335[2]	1.48
Black Gore Creek Near Minturn, CO	116[2]	1.48
ElkRiver Near Milner, CO	3567[2]	2.08

[1]Andrews (1984)
[2]Segura and Pitlick (2010)

For all flow variables except mean monthly, the values used in modeling are only those with complete data for all months (Figure 1, all). Some gages were operated seasonally and were used for monthly flows in which the completeness criteria were met (Figure 1, seasonal).

The predictor variables considered for models of each of the flow metrics in Table 1 describe watershed topography, geology, climate, land cover, soil, and hydrologic region. The variable names and descriptions are given in Table 3.

For topography, we included drainage area, mean watershed elevation, dominant aspect, and slope, the same variables used in CSUFlow18. We added the fraction of drainage area with slopes above 30% to represent the influence of steep slopes on flow routing, and we added northness and fraction of drainage area with northerly aspects. CSUFlow18 used only dominant aspect in eight bins (N, NW, NE, S, SW, SE, W, E), whereas the new variables have continuous values, not divided into bins.

Climate variables in CSUFlow18 were mean annual precipitation (PRISM; Daly, 2013), mean annual potential evapotranspiration (GridMET; Abatzoglou, 2013), and mean annual snow persistence (Hammond et al., 2017). We included these same variables, but we changed the data source for precipitation to Daymet because the Daymet dataset also includes simulated snow water equivalent. From Daymet, we also added mean monthly values of precipitation (all months), mean monthly maximum precipitation, mean snow water equivalent (January-June), and mean annual peak snow water equivalent. Consistent with CSUFlow18, we obtain the estimate of mean annual potential evaporation from the mean annual grass reference evapotranspiration provided in GridMET. This represents the potential for water loss to the atmosphere if vegetation is not water-limited and is a standard choice for representing potential evapotranspiration. Gridded climate products do not include evapotranspiration for variable vegetation types and heights. Also consistent with CSUFlow18, we used the mean annual snow persistence from MODIS satellite snow cover, but the dataset is updated through water year 2020 (Hammond, 2020). Additionally we included the fraction of drainage area above a mean annual snow persistence of 60%, which is the area of the seasonal snow zone. This variable represents the likely area that would contribute snowmelt runoff to the stream.

CSUFlow18 represented geology as a categorical variable with the following categories: permeable sedimentary, impermeable sedimentary, volcanic, impermeable metamorphic, permeable metamorphic, intrusive, modern alluvium/colluvium, glacial/glacial drift. For the updated models we reduced the categories to sedimentary clastic (shale, siltstone, sandstone, conglomerate); sedimentary chemical (limestone, dolomite, evaporite); volcanic (extrusive); intrusive; metamorphic, and unconsolidated (alluvium, colluvium, glacial). The category that covers the largest percent of watershed area is selected.

We initially tried to develop CSUFlow25 models without including hydrologic region because this variable (used in CSUFlow18 and StreamStats) does not have a physical meaning or clear justification for regional boundaries. However, some models performed better when including a hydrologic region predictor variable. The hydrologic regions in CSUFlow18 were the same as those for USGS StreamStats (Capesius and Stephens, 2009) (Figure 2a), but for the model updates we chose to modify the regions somewhat (Figure 2b). The original plains hydrologic region included several areas with steep slopes and higher elevations, so we updated the plains region boundary to include only areas with elevation <2,000 m. This change restricted the plains region to flatter sloped areas. The Front Range slopes that had previously been in the plains hydrologic region moved into the central and southcentral regions. The southcentral region includes both those east-draining Front Range watersheds as well as west-draining watersheds that enter the San Luis Valley. Next, the northwest hydrologic region had very low sample size with the original boundaries, so we expanded it to include the Yampa River basin. The southwest hydrologic region had bisected the San Juan mountains, such that watersheds that were close to one another would end up in two different hydrologic regions. For this reason, we expanded the boundary of the southwest hydrologic region north to the Colorado River and east to the Rio Grande. The remaining area is assigned to the central hydrologic region. Watersheds in the dataset that were outside Colorado were assigned to the nearest hydrologic region.

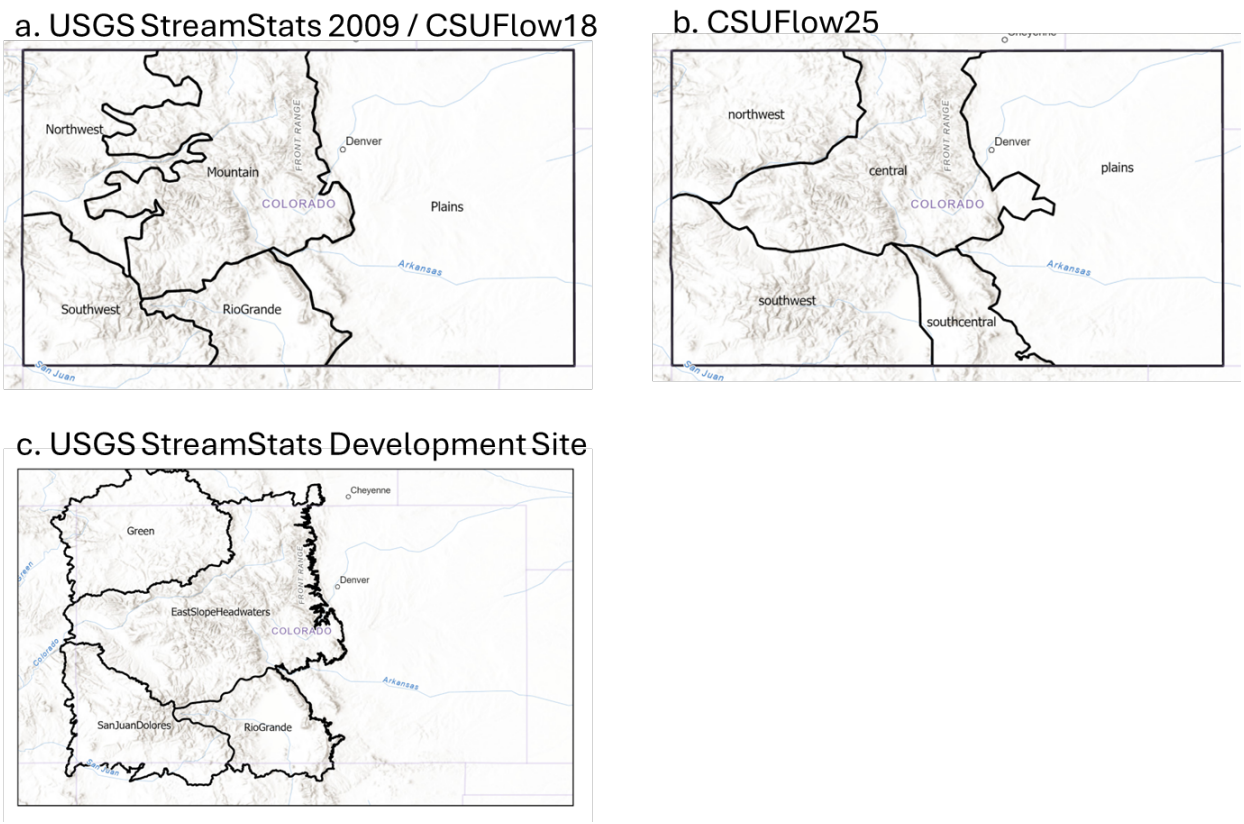

Figure 2. Hydrologic region boundaries from USGS StreamStats 2009 version (a) used in CSUFlow18; new hydrologic region boundaries (b) used in CSUFlow25, and (c) hydrologic regions used in the StreamStats development site (https://test.streamstats.usgs.gov/nss-dev/).

We also added land cover and soil predictor variables; these types of predictors were not part of CSUFlow18. The land cover types are from the National Land Cover Dataset and represent the percent of drainage area covered by major land cover categories (grassland/herbaceous, shrub, forest, agriculture, impervious). Additionally, we included road density because of the influence roads can have on routing water to streams. For soil we included percent sand, percent clay, depth to bedrock, and depth to water table, all variables compiled in the StreamCat dataset.

Table 3. Predictor variables considered for CSUFlow25 models.

Variable ID	Name	Type	Units	Source
area	Watershed drainage area	TOPOGRAPHY	km^2	Gesch et al. (2018), 30-m
elevation	Mean watershed elevation		m	
slope	Mean slope of all grid cells in watershed		fraction	
slope30	Fraction drainage area with slope > 0.3		fraction	
aspect	N, NW, NE, S, SW, SE, E, W		categorical	
northness	Mean northness, computed as the sine of slope multiplied by cosine of aspect		fraction	
north_fraction	Fraction of drainage area with slopes facing north, northwest, or northeast		fraction	
Pann	Mean annual precipitation	CLIMATE	mm	Daymet
Pjan - Pdec	Mean monthly precipitation from Jan - Dec		mm	
Ppeak	Maximum monthly precipitation, averaged over all years		mm	
SWEmean	Mean annual snow water equivalent		mm	
SWEpeak	Mean annual peak snow water equivalent		mm	
SWEjan - SWEjun	Mean monthly snow water equivalent from Jan - Jun		mm	
SP	Mean annual snow persistence (2001-2020)		percent	Hammond (2020)
area60	Fraction of drainage area in the seasonal snow zone, mean annual snow persistence >60%		fraction	
PETann	Mean annual grass reference evapotranspiration		mm	Abatzoglou (2013)
grass, shrub, forest, agriculture	Percent of drainage area with grassland/herbaceous, shrubland, forest, or agriculture land cover	LANDCOVER	percent	NLCD 2019 (Dewitz 2021)
Impervious	Percent impervious surface in drainage area		percent	
Road	Density of roads over drainage area		km/km^2	US Census Bureau (2024)

Variable ID	Name	Type	Units	Source
Sand, clay	Mean percent sand or clay content	soil	percent	StreamCat (Hill et al. 2016)
Bedrock	Mean depth to bedrock		mm	
WaterTable	Mean depth to water table		mm	
Permeability	Mean permeability of soil		cm/hr	
geology	Dominant bedrock type	geology	categorical	Horton et al. (2017)
region	Hydrologic region	region	categorical	-

3. Modeling

3.1. Methods

3.1.1. Model development

We developed multiple linear regression (MLR) models for predicting each of the streamflow variables (Table 1), using the predictor variables in Table 3. First, we addressed multicollinearity among predictor variables using pairwise Pearson correlation, where coefficients ≥ 0.85 were considered highly correlated. The variable with the weaker absolute correlation to the target variable was removed, following the approach of Eurich et al. (2021). Monthly flow metrics were modeled using a reduced set of climate predictors. Each month could only use precipitation for the current month or up to three months prior. January through June could use SWE from the current month or prior months, whereas later months (July - Dec) could only use peak SWE. All other streamflow metrics could draw from the full predictor set.

All streamflow variables were square-root transformed prior to model fitting to best meet the MLR modelling assumption of equal variance, but predictions were back-transformed for performance evaluation. An exhaustive subset selection procedure was used to identify the best-performing combination of up to n/15 predictor groups (where n is the number of observations).

We tried random forest modeling as well, but this approach had problems with over-fitting. Other machine learning techniques considered for the new models proved to be unsuitable for the size of our dataset, so we decided to keep with MLR, the same approach used in CSUFlow18. Initial model tests indicated that Luning Arroyo and Cement Creek at Silverton were extreme outliers in flow conditions, so we removed those sites from the model development dataset.

To assess model generalizability, we employed 5-fold cross-validation using the caret package. Cross-validation is a statistical technique that splits the dataset into multiple subsets (or “folds”), trains the model on some folds while testing it on the remaining fold, and repeats this process to provide a more robust estimate of how well the model will perform on unseen data. This approach allows for evaluation of model performance beyond the training dataset by randomly rotating which portion of the data is held out for testing.

To evaluate model performance for training and cross-validation, we used the Nash-Sutcliffe coefficient of efficiency (NSE) and the percent bias (PBIAS).

3.1.2. Comparison to other models

We compared the performance of the new models to CSUFlow18 and the new development version of StreamStats (USGS) for mean annual and mean monthly flows. For CSUFlow18, these tests used the hydrologic region, slope and aspect data developed for CSUFlow18, with all other inputs coming from the new dataset. We used the old slope and aspect data because the updated slope and aspect rasters for CSUFlow25 were somewhat different from those used previously, and this affected the performance of the models.

The new StreamStats models use as inputs the drainage area (DRNAREA, mi^2), mean slope (ALTBSLDEM, %), and mean annual precipitation (PRECIP, in), which are also potential predictors in CSUFlow25 models. Additionally the USGS models used minimum elevation (ALTOUTELEV, ft), maximum elevation (ALTELEVMAX, ft), and relief (ALTRELIEF, ft), which we assumed was the elevation difference between minimum and maximum. USGS models used latitude and longitudes of the watershed centroids (LAT_CENT, LONG_CENT, decimal degrees); mean April 1 snow water equivalent (APR1_SWE, in); mean August precipitation (AUGAVPRE, in), and 6-hour 100-year precipitation (ALT6H100Y, in). We ran the USGS models using the batch processing tool on the development site.

The USGS model equations are for four hydrologic regions (Figure 2c) and are as follows:

CO_Mean_Flow_East_Slope_Headwaters_SIR_2023_XXXX	
QA =	$10^{-0.704} \cdot DRNAREA^{0.793} \cdot 10^{(0.00518 \cdot ALTBSLDEM + 0.0000642 \cdot ALTRELIEF + 0.0459 \cdot APR1\_SWE)}$

CO_Mean_Flow_East_Slope_Headwaters_SIR_2023_XXXX	
Q1 =	$10^{-1.61} \cdot DRNAREA^{0.773} \cdot 10^{(0.000143 \cdot ALTRELIEF + 0.0440 \cdot APR1\_SWE)}$
Q2 =	$10^{1.21} \cdot DRNAREA^{0.847} \cdot 10^{(-0.0679 \cdot LAT\_CENT + 0.000103 \cdot ALTRELIEF + 0.0364 \cdot APR1\_SWE)}$
Q3 =	$10^{-0.900} \cdot DRNAREA^{0.906} \cdot 10^{(0.0000646 \cdot ALTRELIEF + 0.0166 \cdot PRECIP - 0.228 \cdot ALTI6H100Y)}$
Q4 =	$10^{0.224} \cdot DRNAREA^{0.960} \cdot 10^{(-0.0000664 \cdot ALTOUTELEV + 0.0215 \cdot PRECIP - 0.265 \cdot ALTI6H100Y)}$
Q5 =	$10^{-0.259} \cdot DRNAREA^{0.933} \cdot 10^{(0.0111 \cdot PRECIP + 0.0332 \cdot APR1\_SWE)}$
Q6 =	$10^{16.4} \cdot DRNAREA^{0.690} \cdot 10^{(0.156 \cdot LONG\_CENT + 0.000127 \cdot ALTRELIEF + 0.0651 \cdot APR1\_SWE)}$
Q7 =	$10^{-2.06} \cdot DRNAREA^{0.780} \cdot 10^{(0.000118 \cdot ALTELEVMAX + 0.0130 \cdot ALTBSLDEM + 0.0517 \cdot APR1\_SWE)}$
Q8 =	$10^{-2.21} \cdot DRNAREA^{0.807} \cdot 10^{(0.000101 \cdot ALTELEVMAX + 0.00862 \cdot ALTBSLDEM + 0.0217 \cdot PRECIP)}$
Q9 =	$10^{-1.25} \cdot DRNAREA^{0.707} \cdot 10^{(0.00750 \cdot ALTBSLDEM + 0.00013 \cdot ALTRELIEF + 0.0374 \cdot APR1\_SWE)}$
Q10 =	$10^{-1.06} \cdot DRNAREA^{0.700} \cdot 10^{(0.000144 \cdot ALTRELIEF + 0.0333 \cdot APR1\_SWE)}$
Q11 =	$10^{-1.28} \cdot DRNAREA^{0.749} \cdot 10^{(0.000140 \cdot ALTRELIEF + 0.0363 \cdot APR1\_SWE)}$
Q12 =	$10^{-1.42} \cdot DRNAREA^{0.763} \cdot 10^{(0.000135 \cdot ALTRELIEF + 0.0383 \cdot APR1\_SWE)}$

CO_Mean_Flow_Green_River_SIR_2023_XXXX	
QA =	$10^{21.5} \cdot DRNAREA^{0.753} \cdot 10^{(0.241 \cdot LONG\_CENT + 0.000305 \cdot ALTELEVMAX + 0.587 \cdot ALTI6H100Y)}$

CO_Mean_Flow_Green_River_SIR_2023_XXXX	
Q1 =	$10^{13.4} \cdot DRNAREA^{0.792} \cdot 10^{(0.164 \cdot LONG\_CENT + 0.000273 \cdot ALTELEVMAX + 0.0295 \cdot ALTBSLDEM)}$
Q2 =	$10^{13.9} \cdot DRNAREA^{0.843} \cdot 10^{(0.165 \cdot LONG\_CENT + 0.000229 \cdot ALTELEVMAX + 0.0277 \cdot ALTBSLDEM)}$
Q3 =	$10^{23.5} \cdot DRNAREA^{1.22} \cdot 10^{(0.237 \cdot LONG\_CENT + 0.504 \cdot AUGAVPRE)}$
Q4 =	$10^{20.1} \cdot DRNAREA^{1.23} \cdot 10^{(0.534 \cdot LAT\_CENT + 0.407 \cdot LONG\_CENT + 0.792 \cdot AUGAVPRE)}$
Q5 =	$\left(10^{12.7}\right) \cdot \left(DRNAREA^{1.21}\right) \cdot 10^{(0.805 \cdot LAT\_CENT) + (0.446 \cdot LONG\_CENT) + (1.44 \cdot AUGAVPRE)}$
Q6 =	$10^{-13.7} \cdot DRNAREA^{0.885} \cdot 10^{(0.240 \cdot LAT\_CENT + 0.000276 \cdot ALTELEVMAX + 0.0414 \cdot PRECIP)}$
Q7 =	$10^{-2.44} \cdot DRNAREA^{0.938} \cdot 10^{(0.000109 \cdot ALTRELIEF) + (0.573 \cdot AUGAVPRE) + (0.0603 \cdot APR1\_SWE)}$
Q8 =	$10^{-1.90} \cdot DRNAREA^{1.07} \cdot 10^{(1.05 \cdot AUGAVPRE + 0.0419 \cdot APR1\_SWE - 0.638 \cdot ALTI6H100Y)}$
Q9 =	$10^{-3.44} \cdot DRNAREA^{1.13} \cdot 10^{(0.0228 \cdot ALTBSLDEM + 0.732 \cdot AUGAVPRE + 0.0382 \cdot APR1\_SWE)}$
Q10 =	$10^{-4.36} \cdot DRNAREA^{0.877} \cdot 10^{(0.000242 \cdot ALTELEVMAX + 0.0329 \cdot ALTBSLDEM + 0.0293 \cdot APR1\_SWE)}$
Q11 =	$10^{-3.66} \cdot DRNAREA^{0.903} \cdot 10^{(0.000182 \cdot ALTELEVMAX + 0.0284 \cdot ALTBSLDEM + 0.0276 \cdot APR1\_SWE)}$
Q12 =	$10^{-1.31} \cdot DRNAREA^{1.12} \cdot 10^{(0.558 \cdot AUGAVPRE + 0.0384 \cdot APR1\_SWE - 0.591 \cdot ALTI6H100Y)}$

CO_Mean_Flow_Rio_Grande_SIR_2023_XXXX	
QA =	$10^{21.1} \cdot DRNAREA^{0.839} \cdot 10^{(0.129 \cdot LAT\_CENT + 0.250 \cdot LONG\_CENT + 0.0783 \cdot APR1\_SWE)}$

CO_Mean_Flow_Rio_Grande_SIR_2023_XXXX	
Q1 =	$10^{58.1} \cdot DRNAREA^{0.817} \cdot 10^{(0.544 \cdot LONG\_CENT + 0.0734 \cdot APR1\_SWE - 0.579 \cdot ALTI6H100Y)}$
Q2 =	$10^{50.9} \cdot DRNAREA^{0.842} \cdot 10^{(0.478 \cdot LONG\_CENT + 0.0647 \cdot APR1\_SWE - 0.501 \cdot ALTI6H100Y)}$
Q3 =	$10^{-0.648} \cdot DRNAREA^{0.845} \cdot 10^{(0.0255 \cdot APR1\_SWE)}$
Q4 =	$10^{1.83} \cdot DRNAREA^{0.705} \cdot 10^{(-0.000244 \cdot ALTOUTELEV - 0.00544 \cdot ALTBSLDEM + 0.0772 \cdot APR1\_SWE)}$
Q5 =	$10^{20.6} \cdot DRNAREA^{0.878} \cdot 10^{(0.200 \cdot LONG\_CENT + 0.0000655 \cdot ALTRELIEF + 0.0847 \cdot APR1\_SWE)}$
Q6 =	$10^{25.9} \cdot DRNAREA^{0.789} \cdot 10^{(0.268 \cdot LONG\_CENT + 0.000181 \cdot ALTELEVMAX + 0.0926 \cdot APR1\_SWE)}$
Q7 =	$10^{0.160} \cdot DRNAREA^{0.409} \cdot 10^{(0.000222 \cdot ALTRELIEF + 0.0946 \cdot APR1\_SWE - 0.436 \cdot ALTI6H100Y)}$
Q8 =	$10^{0.274} \cdot DRNAREA^{0.398} \cdot 10^{(0.000187 \cdot ALTRELIEF + 0.067 \cdot APR1\_SWE - 0.393 \cdot ALTI6H100Y)}$
Q9 =	$10^{0.207} \cdot DRNAREA^{0.424} \cdot 10^{(0.000189 \cdot ALTRELIEF + 0.068 \cdot APR1\_SWE - 0.441 \cdot ALTI6H100Y)}$
Q10 =	$10^{28.2} \cdot DRNAREA^{0.815} \cdot 10^{(0.334 \cdot LAT\_CENT + 0.393 \cdot LONG\_CENT + 0.0778 \cdot APR1\_SWE)}$
Q11 =	$10^{49.9} \cdot DRNAREA^{0.739} \cdot 10^{(0.465 \cdot LONG\_CENT + 0.0814 \cdot APR1\_SWE - 0.543 \cdot ALTI6H100Y)}$
Q12 =	$10^{60.6} \cdot DRNAREA^{0.798} \cdot 10^{(0.567 \cdot LONG\_CENT + 0.0785 \cdot APR1\_SWE - 0.590 \cdot ALTI6H100Y)}$

CO_Mean_Flow_San_Juan_Delores_SIR_2023_XXXX	
QA =	$10^{39.5} \cdot DRNAREA^{0.631} \cdot 10^{(0.383 \cdot LONG\_CENT + 0.000175 \cdot ALTELEVMAX)}$

CO_Mean_Flow_San_Juan_Delores_SIR_2023_XXXX	
Q1 =	$10^{42.0} \cdot DRNAREA^{0.811} \cdot 10^{(0.407 \cdot LONG\_CENT + 0.0162 \cdot ALTBSLDEM + 0.000117 \cdot ALTRELIEF)}$
Q2 =	$10^{33.5} \cdot DRNAREA^{0.834} \cdot 10^{(0.324 \cdot LONG\_CENT + 0.0113 \cdot ALTBSLDEM + 0.000083 \cdot ALTRELIEF)}$
Q3 =	$10^{27.7} \cdot DRNAREA^{0.712} \cdot 10^{(0.270 \cdot LONG\_CENT + 0.000106 \cdot ALTELEVMAX)}$
Q4 =	$10^{14.4} \cdot DRNAREA^{0.701} \cdot 10^{(0.171 \cdot LONG\_CENT + 0.000200 \cdot ALTELEVMAX + 0.770 \cdot ALTI6H100Y)}$
Q5 =	$10^{29.7} \cdot DRNAREA^{0.561} \cdot 10^{(0.309 \cdot LONG\_CENT + 0.000261 \cdot ALTELEVMAX + 0.502 \cdot ALTI6H100Y)}$
Q6 =	$10^{52.3} \cdot DRNAREA^{0.483} \cdot 10^{(0.509 \cdot LONG\_CENT + 0.000289 \cdot ALTELEVMAX)}$
Q7 =	$10^{43.8} \cdot DRNAREA^{0.964} \cdot 10^{(0.419 \cdot LONG\_CENT + 0.0322 \cdot ALTBSLDEM)}$
Q8 =	$10^{36.7} \cdot DRNAREA^{1.04} \cdot 10^{(0.353 \cdot LONG\_CENT + 0.0233 \cdot ALTBSLDEM)}$
Q9 =	$10^{44.4} \cdot DRNAREA^{1.03} \cdot 10^{(0.425 \cdot LONG\_CENT + 0.0211 \cdot ALTBSLDEM)}$
Q10 =	$10^{42.1} \cdot DRNAREA^{0.902} \cdot 10^{(0.401 \cdot LONG\_CENT + 0.0195 \cdot ALTBSLDEM)}$
Q11 =	$10^{44.7} \cdot DRNAREA^{0.719} \cdot 10^{(0.427 \cdot LONG\_CENT + 0.0140 \cdot ALTBSLDEM + 0.000110 \cdot ALTRELIEF)}$
Q12 =	$10^{47.7} \cdot DRNAREA^{0.745} \cdot 10^{(0.458 \cdot LONG\_CENT + 0.0147 \cdot ALTBSLDEM + 0.000129 \cdot ALTRELIEF)}$

Equations from https://test.streamstats.usgs.gov/nss-dev/.

The USGS models all predict streamflow in cfs. We converted these values to mm for comparison with our models.

3.1.3. Uncertainty analysis

To evaluate how much flow conditions could differ from the average magnitudes and timing, we also computed mean monthly flow and dates of flow quantiles for the wettest 25% of years and driest 25% of years. We added 95% confidence intervals to the model predictions, so that users of the CSUFlow25 app are able to evaluate the uncertainty of each prediction.

3.2. Results

3.2.1. Model performance

For mean annual and mean monthly flow, the CSUFlow25 models are generally strong for annual and snowmelt runoff season flows and weaker for low flow months (Figures 3-8). Mean annual flow predictions are very good for both CSUFlow25 and CSUFlow18, with more scatter in the predicted vs. observed flow plots for the USGS model (Figure 3). The January and February CSUFlow25 models tend to under-predict at sites with higher winter flows, and this is a problem for the CSUFlow18 and USGS models as well (Figure 4, Figure 8). Performance generally improves as the snowmelt season progresses from March - July for all models (Figure 4, 5, 8), stays strong in August and September, then declines through the fall and winter (Figure 6, 7, 8).

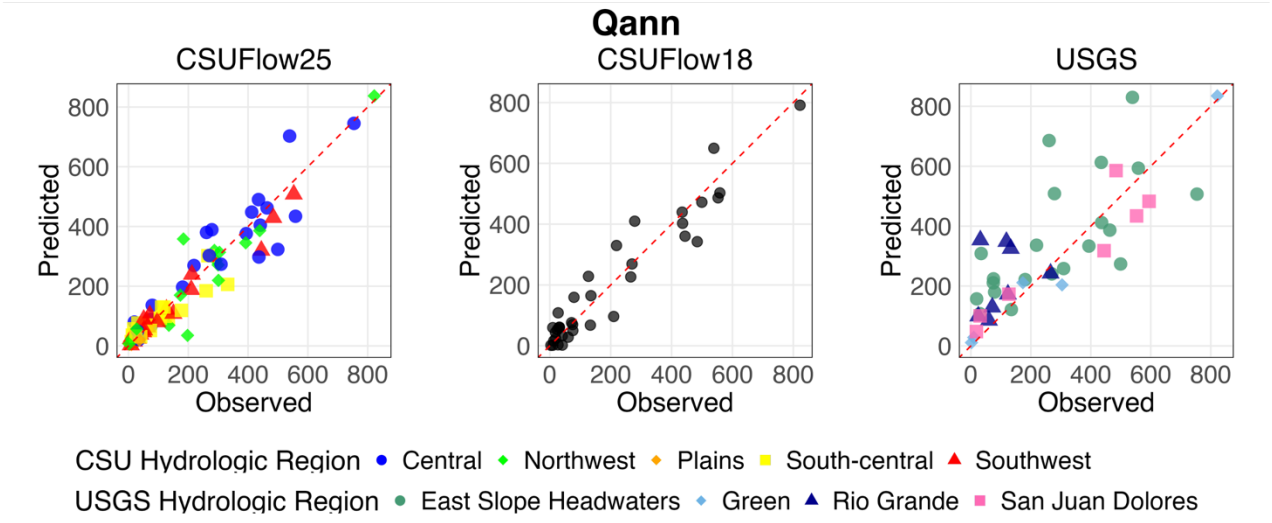

Figure 3. Predicted vs. observed mean annual total flow across the three models compared in this report. Versions of this and the following figures with matching y-axis ranges are in Appendix C.

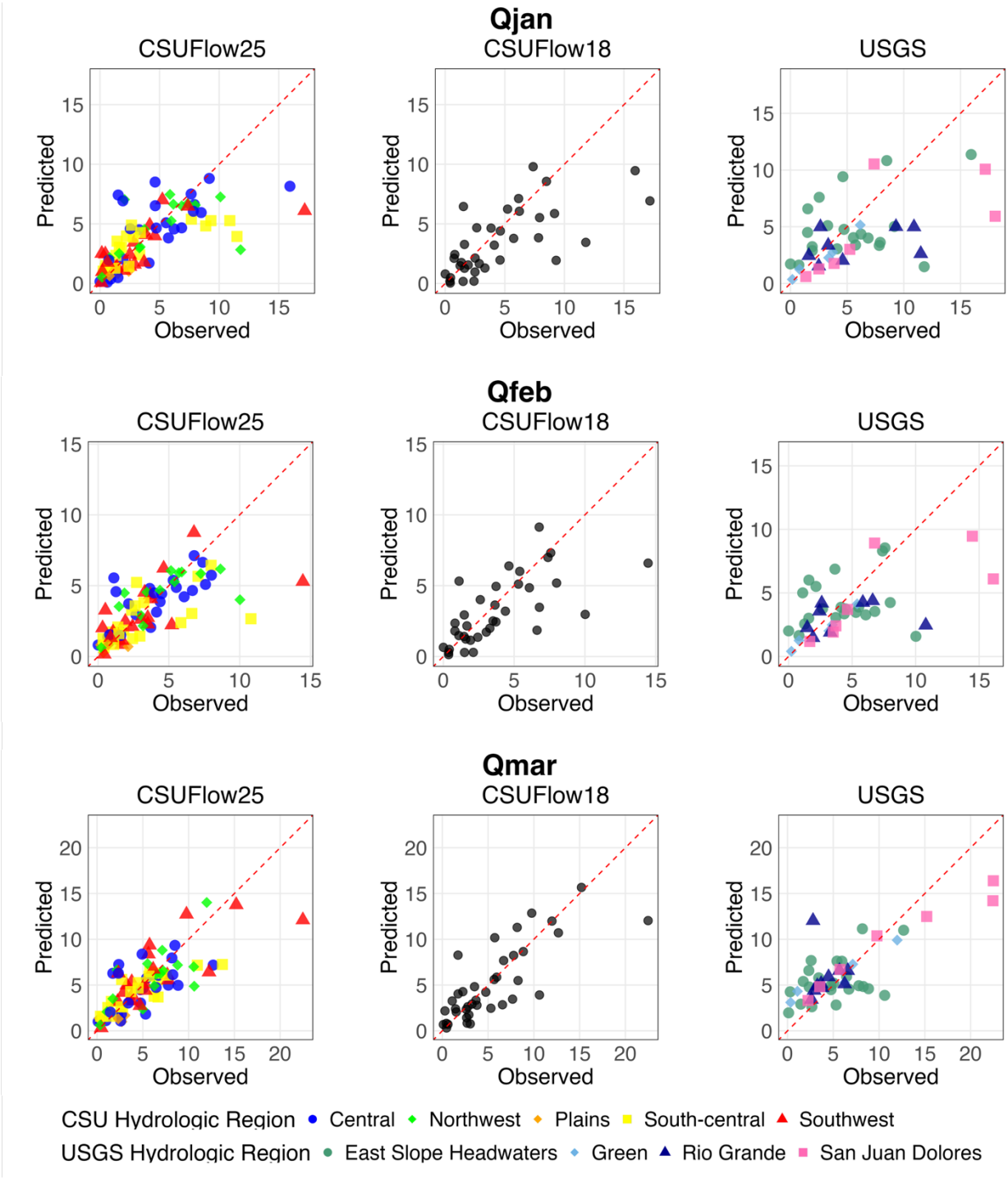

Figure 4. Predicted vs. observed mean flow in January, February, and March across the three models compared in this report.

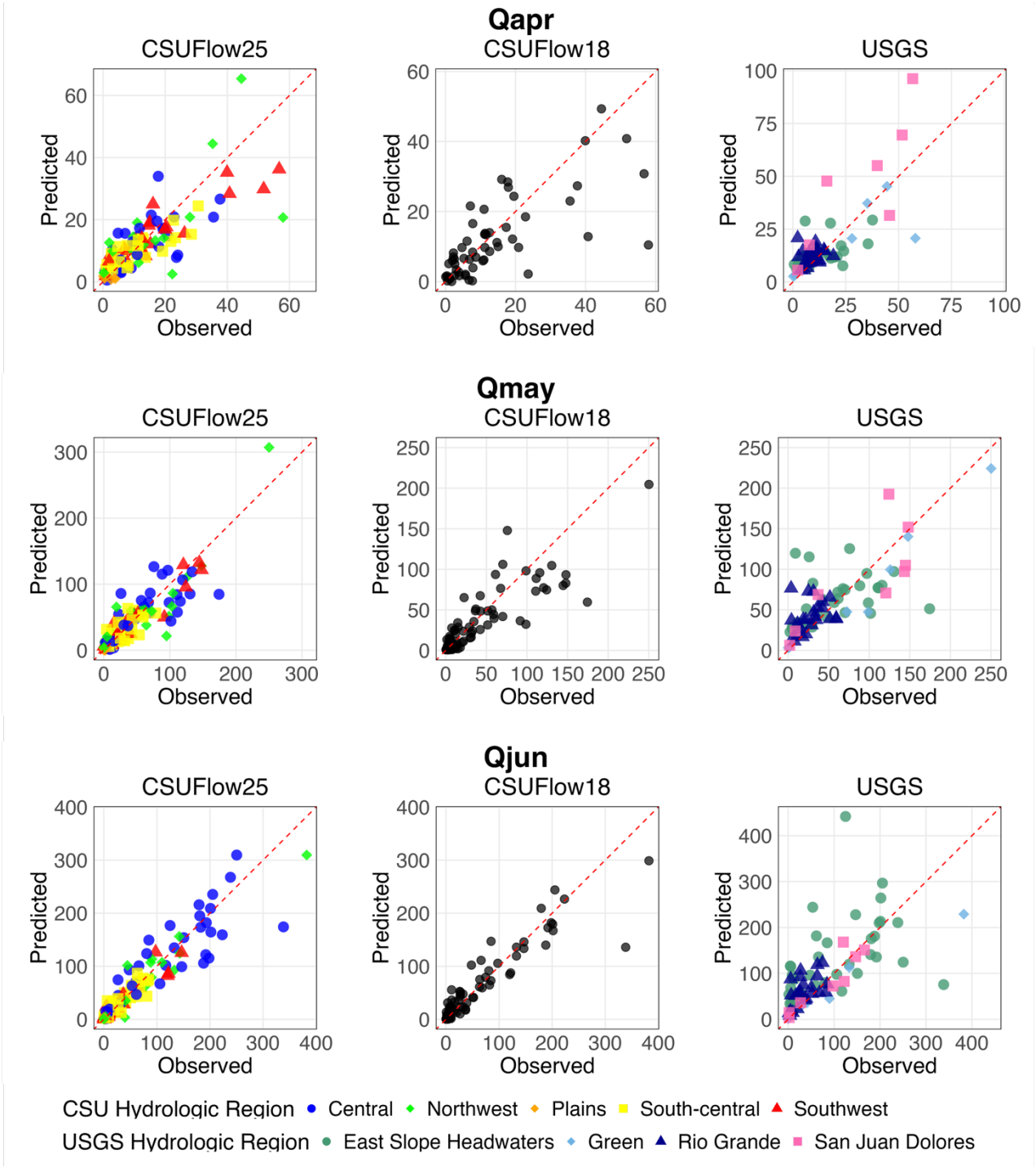

Figure 5. Predicted vs. observed mean flow in April, May, and June across the three models compared in this report.

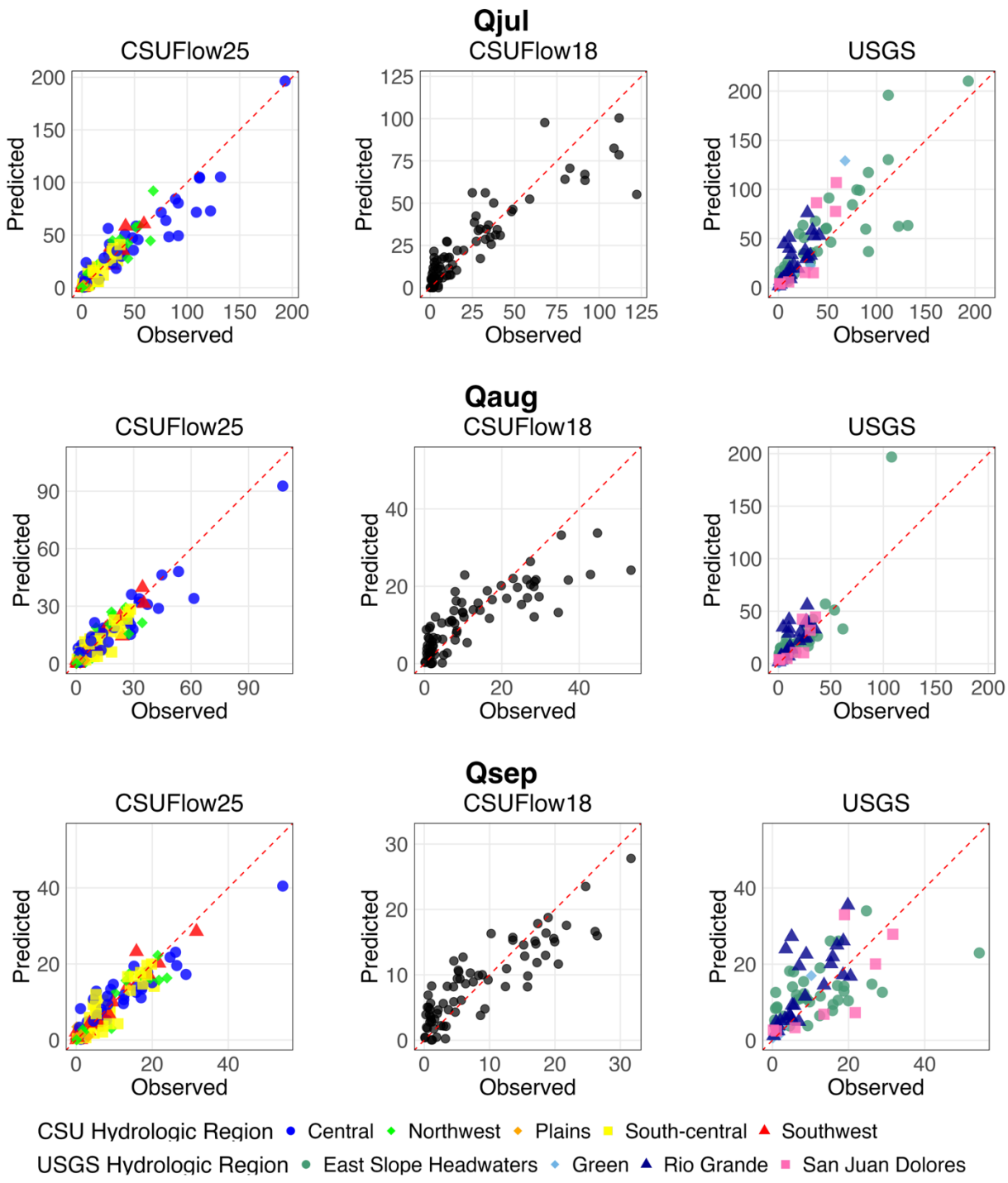

Figure 6. Predicted vs. observed mean flow in July, August, and September across the three models compared in this report.

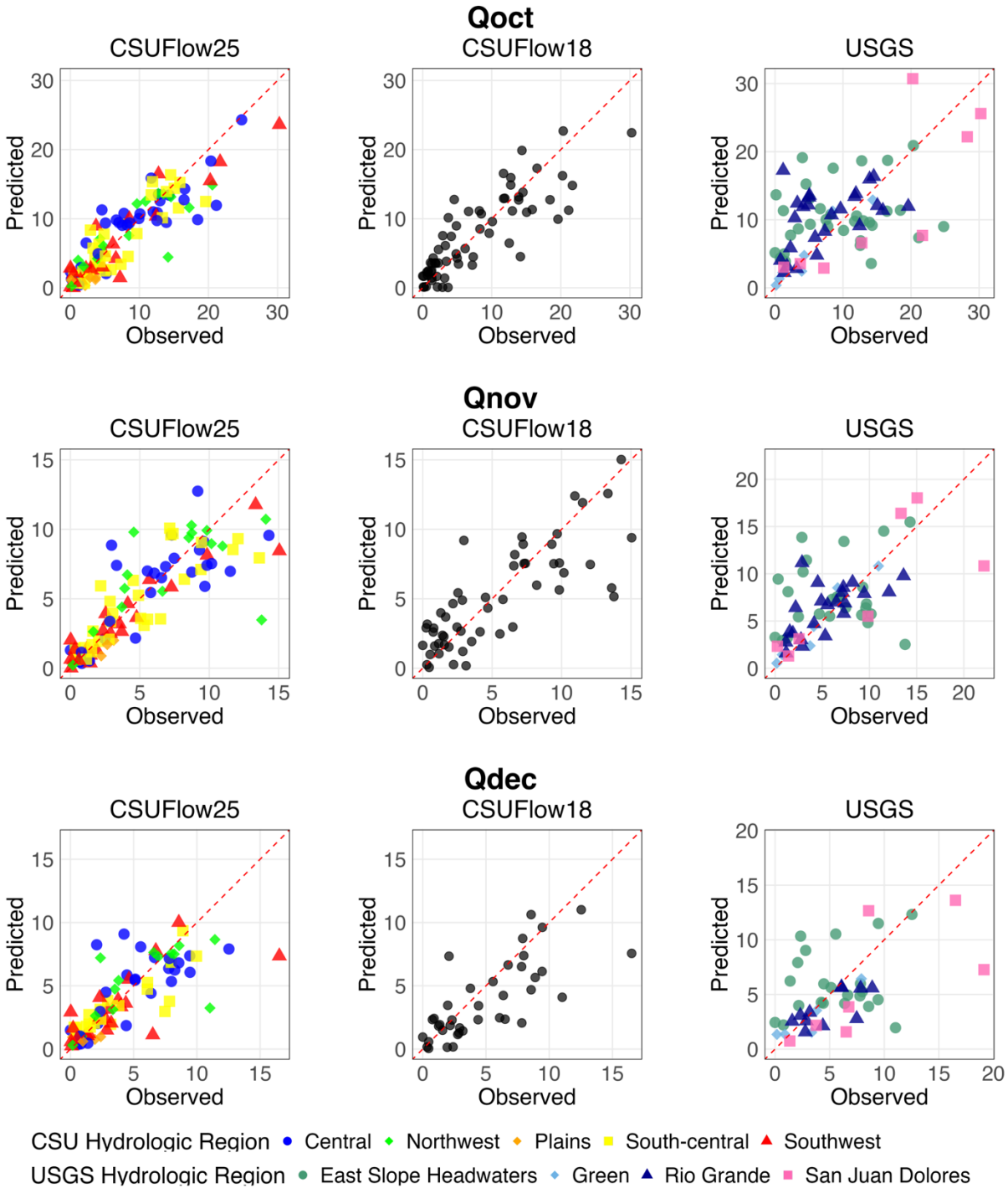

Figure 7. Predicted vs. observed mean flow in October, November, and December across the three models compared in this report.

Summarizing across all the models, CSUFlow25 models performed better than CSUFlow18 for nearly all months (Figure 8). Generally performance of CSUFlow25 models is stronger for the training dataset than

for the cross validation, but these differences are minimal in most months. The USGS models have different performance statistics depending on whether we use the original model predictions (cfs) or convert the cfs values to mm. The USGS models were developed for flow in cfs, and NSE for cfs predictions is stronger than CSUFlow25 for February-May but weaker than CSUFlow25 for all other months. Performance of the USGS models is consistently lower than CSUFlow25 for NSE when flows are converted to mm. PBIAS in the USGS models is greater (absolute value) than CSUFlow25 for all months, meaning the USGS models are more biased, with a tendency to over-predict mean monthly flows, especially during June-November.

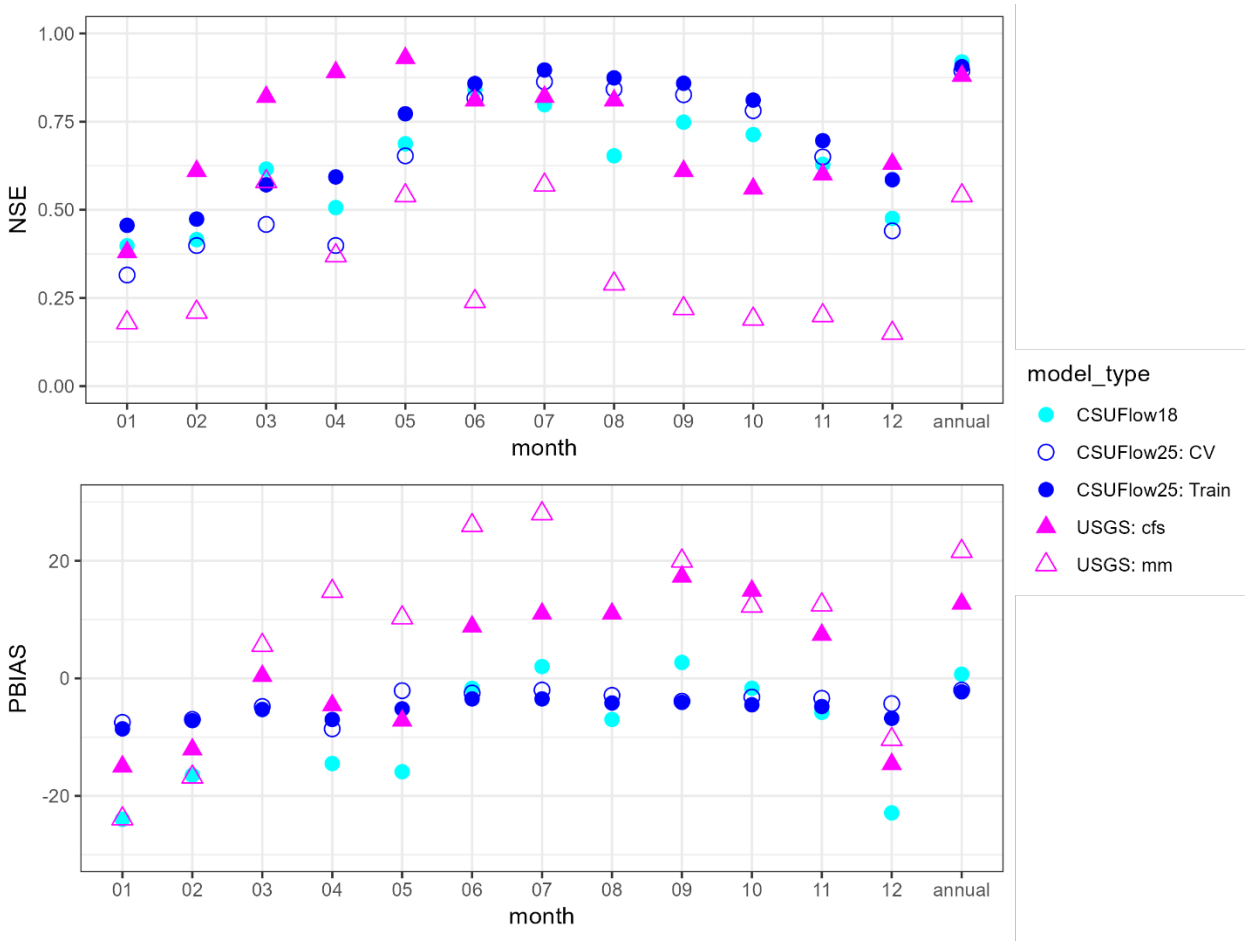

Figure 8. Performance of CSUFlow25 compared to CSUFlow18 and USGS StreamStats (development version) for mean monthly and mean annual flow. NSE is the Nash-Sutcliffe efficiency coefficient; PBIAS is percent bias; CV is cross validation. If a model does not have a point for a given month, this indicates the performance was out of bounds of the graph (worse performance).

The performance of the annual and monthly CSUFlow25 models varied by region (Figure 9). The southwest region had the highest NSE for mean annual flow and most mean monthly flows, followed by the central, southcentral, and northwest regions. The NSE performance was generally poorest for the plains region. PBIAS also varied by region, with generally strongest performance in the central region and poorest in the plains.

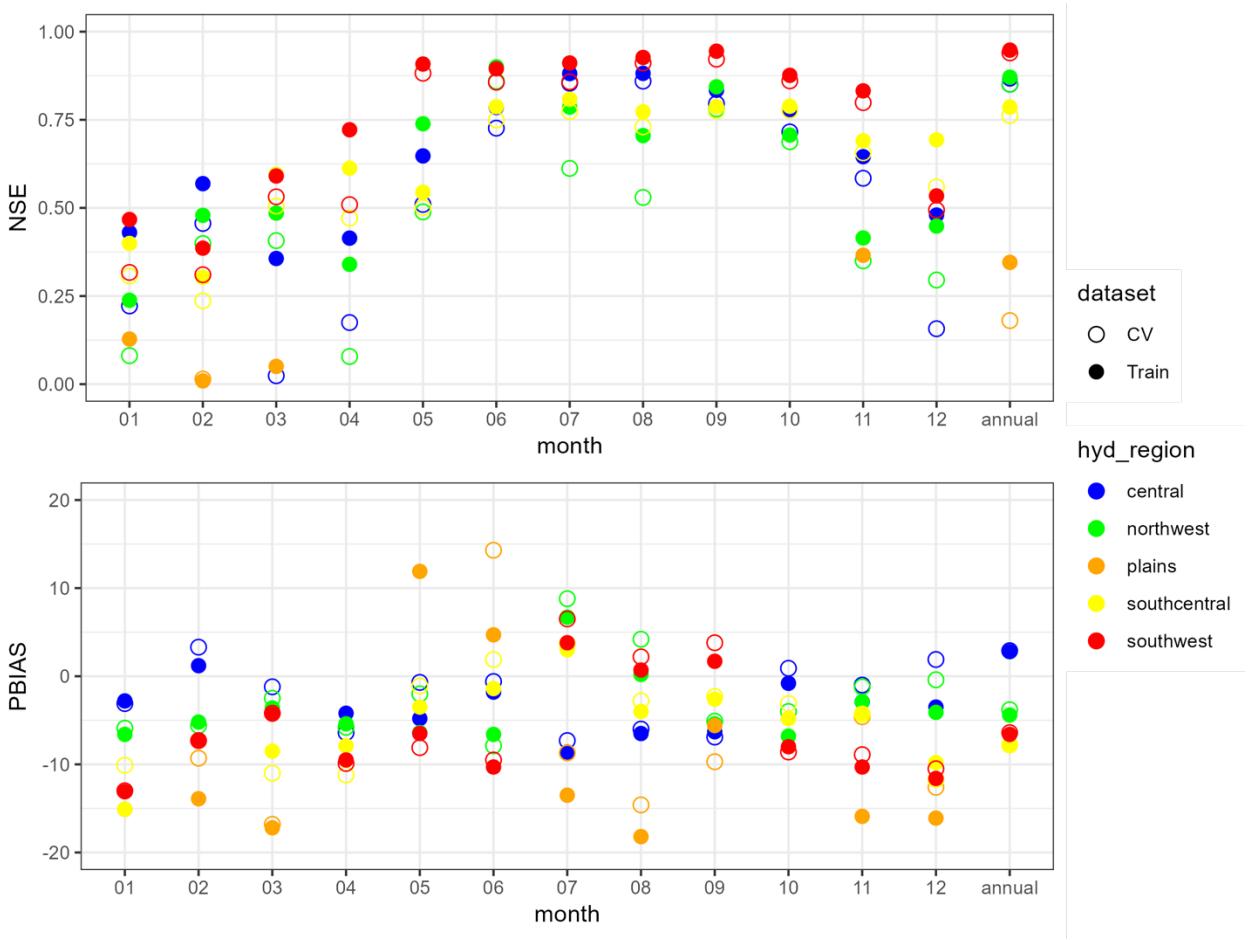

Figure 9. Performance of CSUFlow25 by hydrologic region for mean monthly and mean annual flow. NSE is the Nash-Sutcliffe efficiency coefficient; PBIAS is percent bias; CV is cross validation.

The CSUFlow25 models for high flow (Qmax,Q95) performed well (NSE 0.88-0.91; Figure 10, Table 4), whereas those for low flows (Qmin, Q5) were not as strong (NSE 0.60-0.67). Performance of these models was strongest in the southwest region and weakest in the plains region (Figure 11).

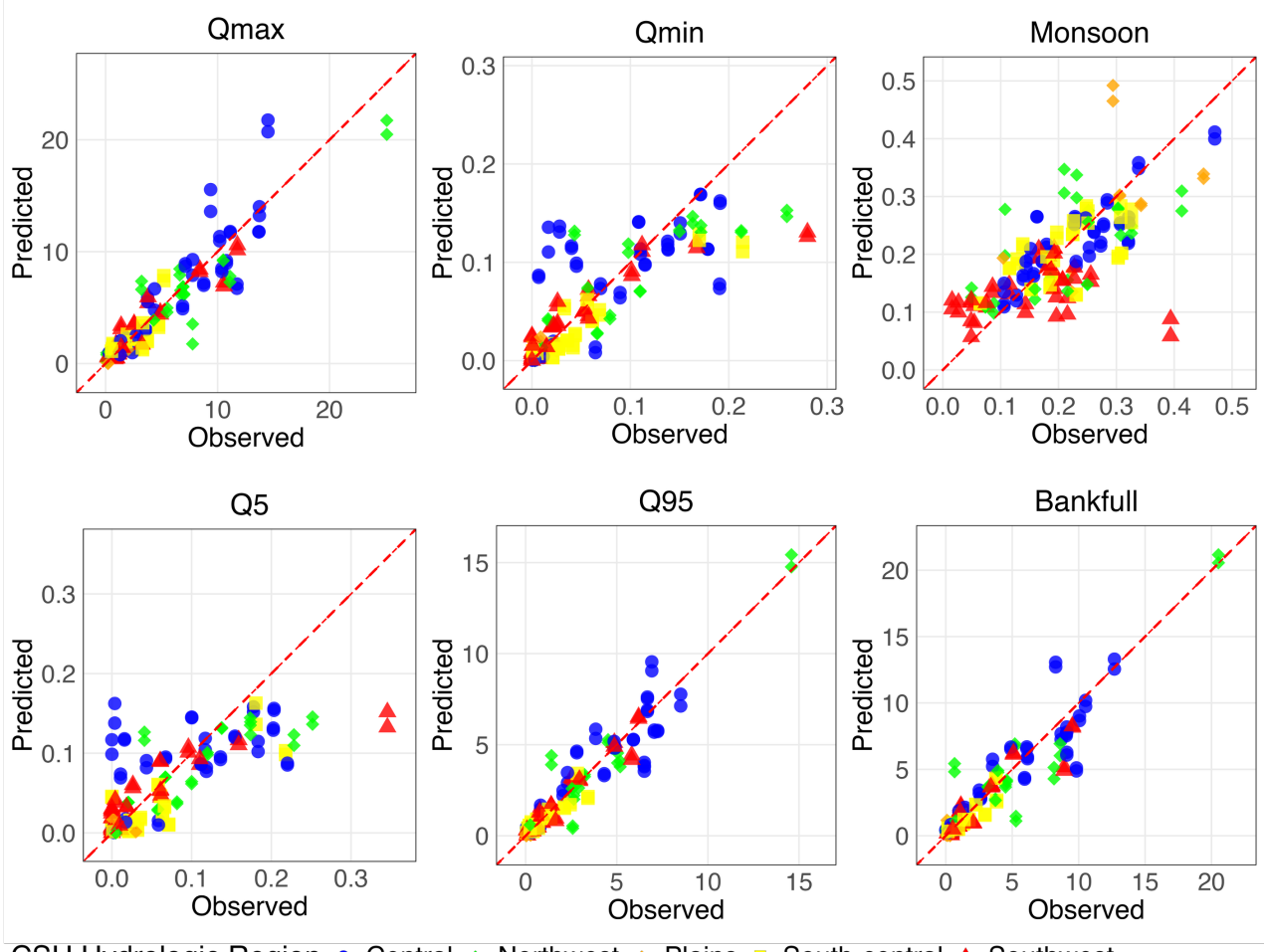

Figure 10. Predicted vs. observed values for CSUflow25 for Qmax, Qmin, monsoon, Q5, Q95, and bankfull.

Table 4. Performance statistics for CSUFlow25 models for high flows, low flows, monsoon flow, and bankfull flow. Values in parentheses are for cross validation.

Variable	**NSE**	**PBIAS**
Qmax	0.88 (0.82)	-2.5 (-1.4)
Q95	0.91 (0.88)	-2.5 (-1.5)
Qmin	0.67 (0.63)	-9.1 (-9.1)
Q5	0.60 (0.54)	-15.1 (-13.6)
monsoon	0.52 (0.35)	-2.9 (-3.3)
bankfull	0.88 (0.86)	-3.9 (-4.0)

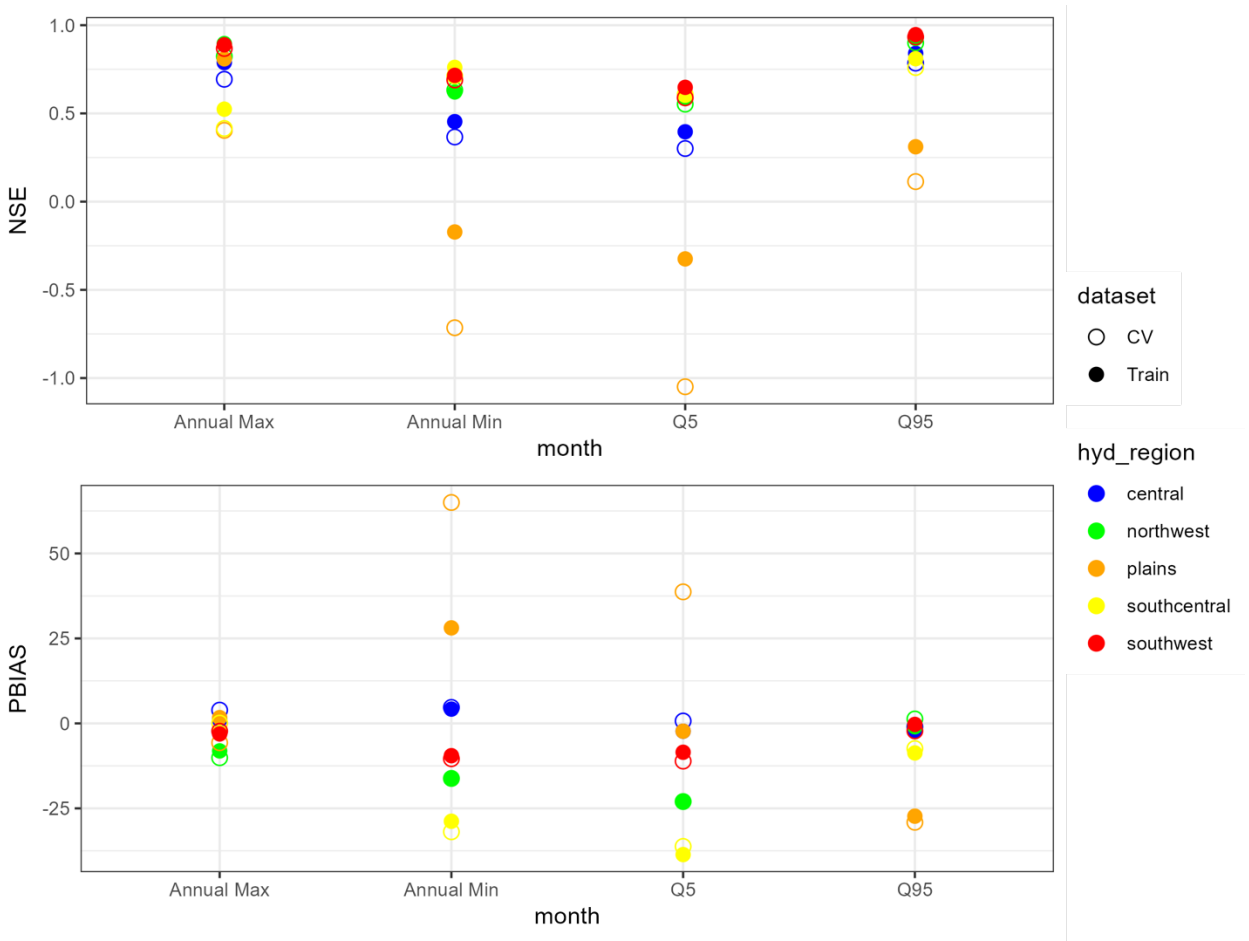

Figure 11. Performance of CSUFlow25 by hydrologic region for high and low flows. NSE is the Nash-Sutcliffe efficiency coefficient; PBIAS is percent bias; CV is cross validation.

The model for fraction of total flow during monsoon months was moderate (NSE 0.52), and it performed best in the central region and worst in the southwest region (Figure 12). Unfortunately, the southwest region is where the monsoon influence is expected to be strongest. In contrast, the model for the 1.5 year return interval flow (bankfull) was very good, with NSE =0.86 and PBIAS -4.0 in cross validation. Performance of this model was strong (NSE>0.75, PBIAS < 10%) in all regions except the plains, where NSE was negative (Figure 13).

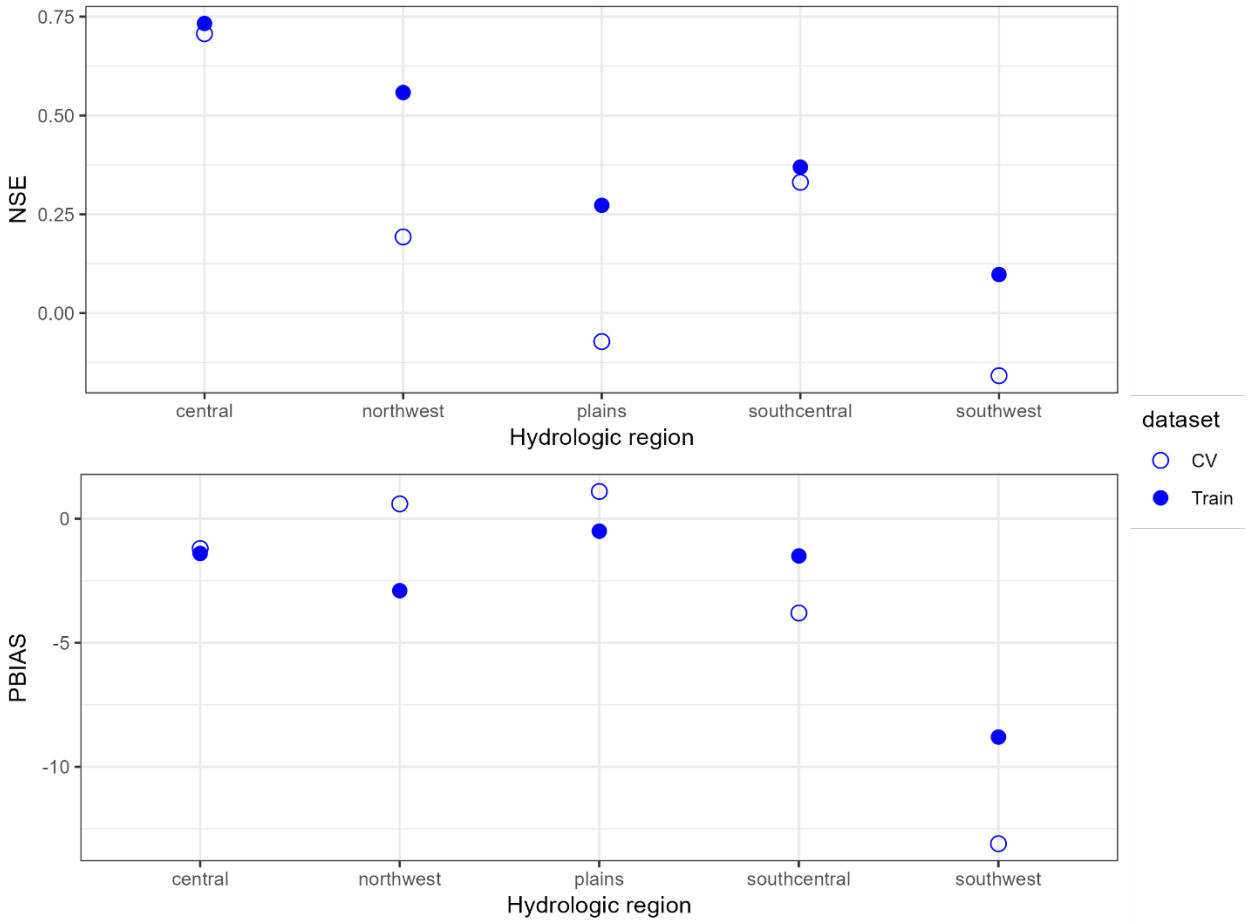

Figure 12. Performance of CSUFlow25 by hydrologic region for the fraction of total flow during the monsoon season. NSE is the Nash-Sutcliffe efficiency coefficient; PBIAS is percent bias; CV is cross validation.

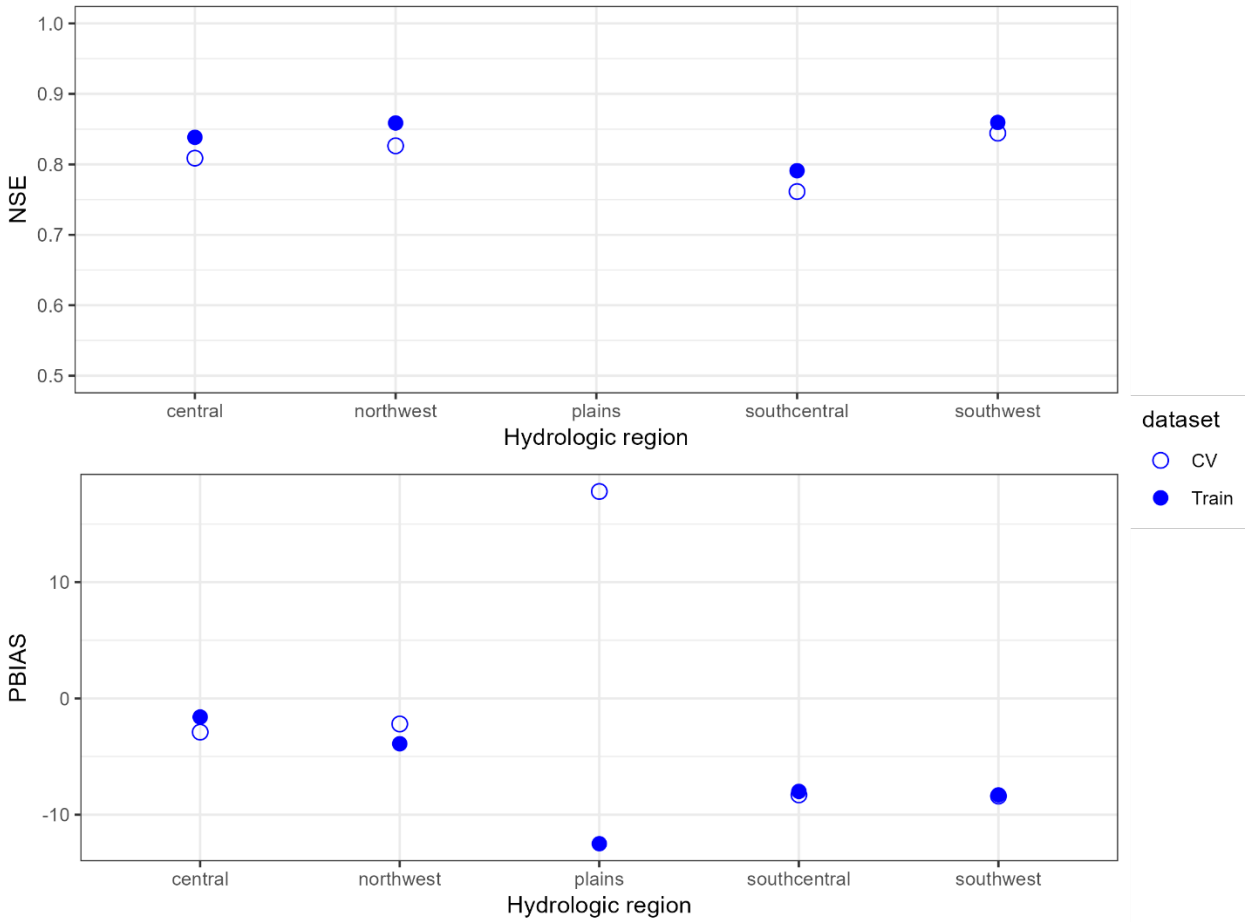

Figure 13. Performance of CSUFlow25 by hydrologic region for the 1.5-year return period (bankfull) flow. NSE is the Nash-Sutcliffe efficiency coefficient; PBIAS is percent bias; CV is cross validation. NSE values for the plain region are negative and not shown in the plot.

Models for flow timing generally exhibit more scatter around the 1:1 line in predicted vs. observed plots (Figure 14). Their performance is very good for PBIAS (<2%), but it is not as strong for NSE (Figure 15). NSE is highest (>0.6) for 20-60% then declines to NSE<0.5 for the later season quantiles. NSE cross validation tests show a substantial decline in performance, meaning that these models are very sensitive to the pool of sites selected. The strong performance in terms of PBIAS compared to NSE is likely due to a relatively even range of scatter on the high and low sides of the 1:1 line (Figure 14). Performance of the timing models is actually strongest in the plains region for NSE and weakest for the southwest and southcentral regions (Figure 16).

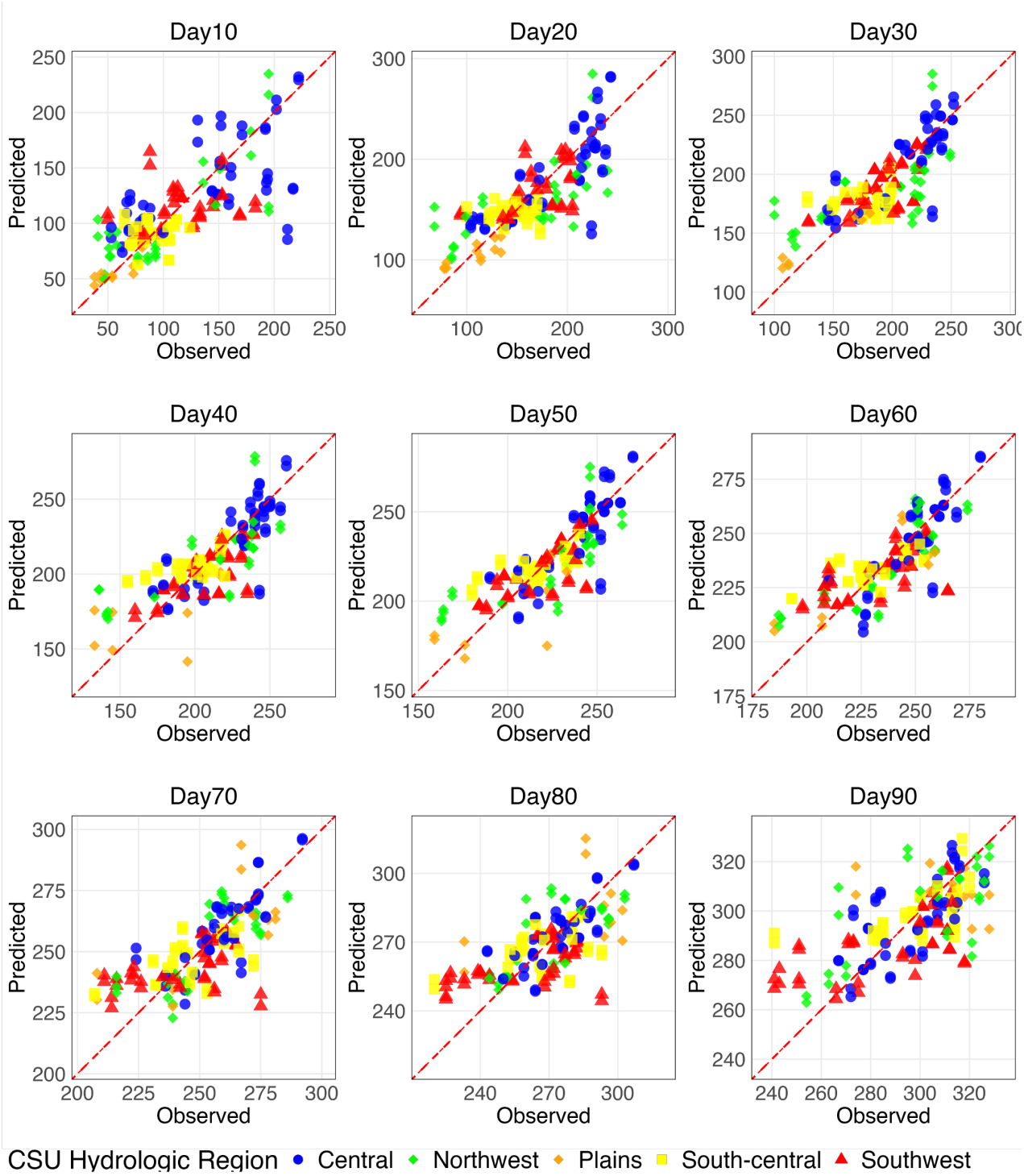

Figure 14. Predicted vs. observed values across the novel flow metrics for the mean date of the 10th, 20th, 30th, 40th, 50th, 60th, 70th, 80th and 90th percentile flows.

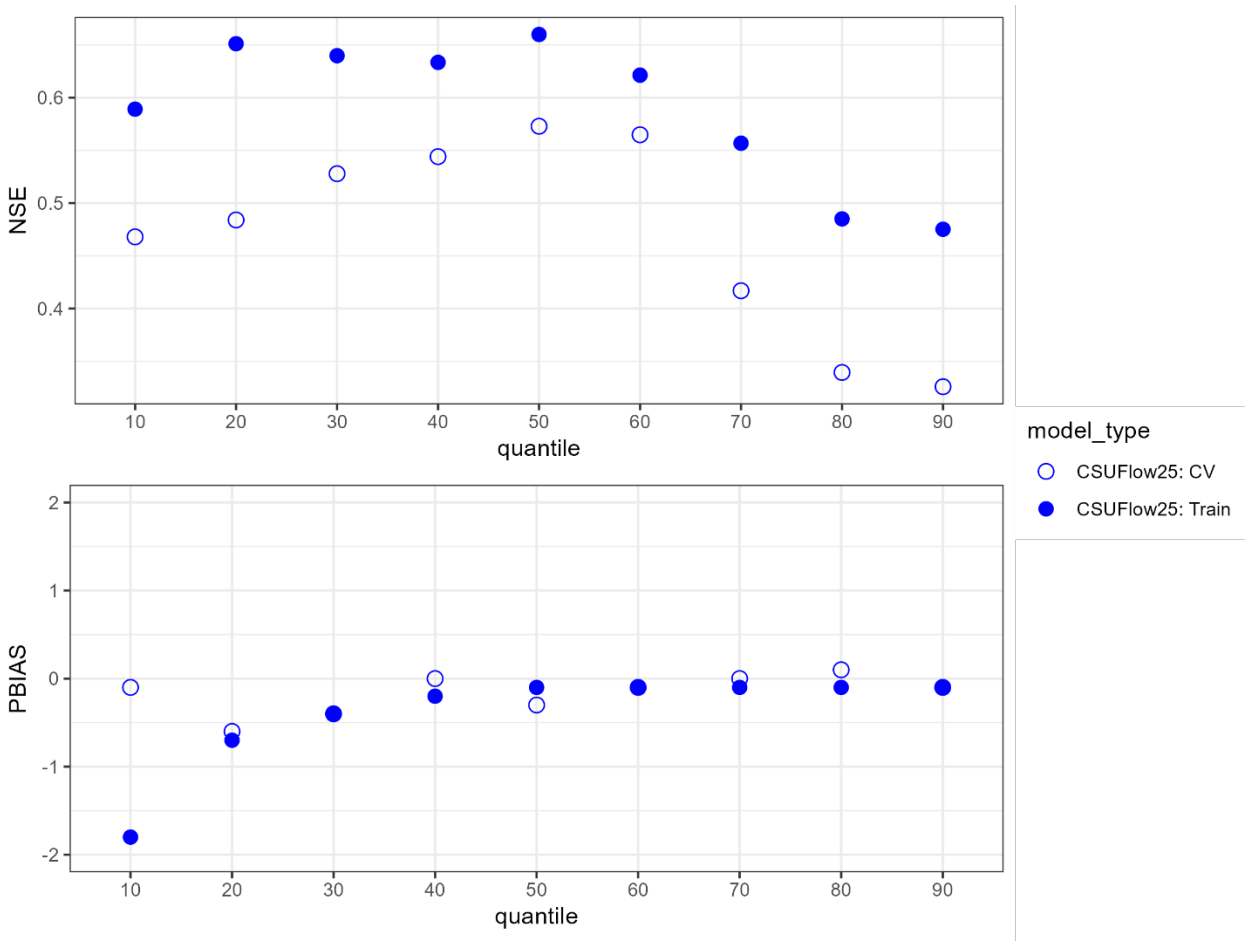

Figure 15. Performance of flow timing models. Quantiles are the percent of water year total flow. NSE is the Nash-Sutcliffe efficiency coefficient, and PBIAS is percent bias. CV is cross-validation.

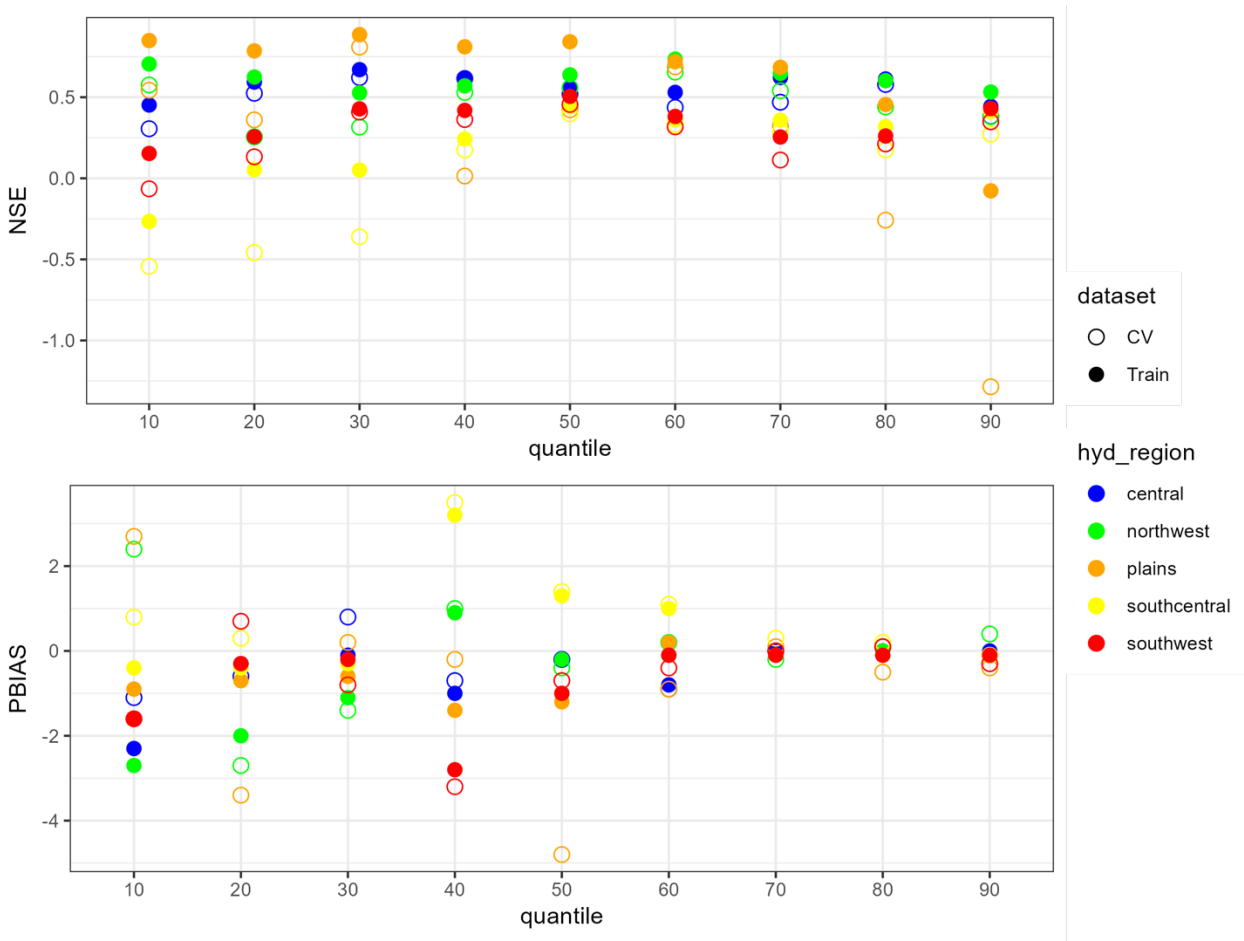

Figure 16. Performance of flow timing models by hydrologic region. Quantiles are the percent of water year total flow. NSE is the Nash-Sutcliffe efficiency coefficient, and PBIAS is percent bias. CV is cross-validation.

3.2.2. Predictor variables

Each of the models selected a different set of predictor variables (Table B1). Some of these reveal seasonal differences in the factors affecting streamflow. For mean monthly flows, the topographic variables selected included dominant aspect, northness, and north fraction for winter months, potentially an indicator of how much snow will be melted vs retained in those months. Mean slope was selected as a predictor for June-December, potentially because of the role of slope in the rate of flow routing to the stream. Percent area of watershed in the seasonal snow zone (area60) was selected as a predictor for September-December, likely because of the influence of high elevations on late-season streamflow.

Climate variables selected for the mean monthly models were mean annual snow persistence (SP) for January-March and one of the SWE variables for May-August. Late season (Sep, Oct) models selected August and/or September precipitation as predictors. Each of these climate variables gives important information about the quantity of water that can reach the stream. The models relied heavily on land cover, particularly shrubland (Feb-Apr and Jul-Dec) and forest (May-Oct). Dominant geology and percent sand were selected for five of the months and water table depth for 7/12 months. Hydrologic region was used in half of the monthly models.

Models for high flows (Qmax, Q95) were surprisingly different in selected predictors. Qmax used hydrologic region, SWEapr, Pmay, agriculture, and sand, whereas Q95 used SWEmar, forest, grassland, road density, and water table depth. Qmax is an annual mean value, which may rely more on snow accumulation and precipitation, whereas Q95 represents the highest flows, which may happen due to overland flow over roads. The low flow models (Qmin, Q5) were more consistent in predictor variable selection. Both used percent area in the seasonal snow zone, precipitation in May or June, shrubland, sand, and permeability. This indicates that the low flows are affected by contributions from high elevation snowmelt and differ depending on soil properties.

Models for the flow quantiles used hydrologic region for the early (10-30%) and late (70-90%) quantiles, an indication that the predictor variables we included did not account for all the factors that affect flow timing. The models used SWEapr for the 30-40% quantiles; SWEmay for 50-60%, and SWEjun for 70-90%, reflecting the role of snowmelt in the timing of streamflow. Psep was used for 10-60% quantiles and Paug for 50-90% quantiles, showing the importance of late summer precipitation for baseflow. Only two of the quantile models used a land cover variable (agriculture for 40-50%), and half of the models used percent sand.

Predictors for the fraction of flow during the monsoon were similar to those for the later flow quantiles: hydrologic region, SWEjun, Paug, sand, and water table depth. The monsoon model did not have strong performance, but it did at least pick out the importance of precipitation during the monsoon season (Paug) for monsoonal streamflow.

Finally, predictors for the 1.5 year return period flow (bankfull) were SWEmar, Pmay, road density, water table depth, and percent sand. These are similar to the predictors for Q95, probably because the bankfull flow is a relatively high flow rate.

3.2.3. Differences for wet and dry years

To evaluate the range of variability that can be expected for the flow metrics, we compared the mean values used in modeling to the values for the wettest years (top 25% of annual flow) and driest years (bottom 25% of annual flow) (Figure 17). The wet years had a median monthly flow that was 15% higher than average during the winter months (Nov-Jan), increasing to 73% higher flow during June. The dry years had median monthly flow 17-19% lower than average during winter months, increasing to 69% lower than average in June. This indicates that the wet-dry year differences were greatest during the snowmelt months.

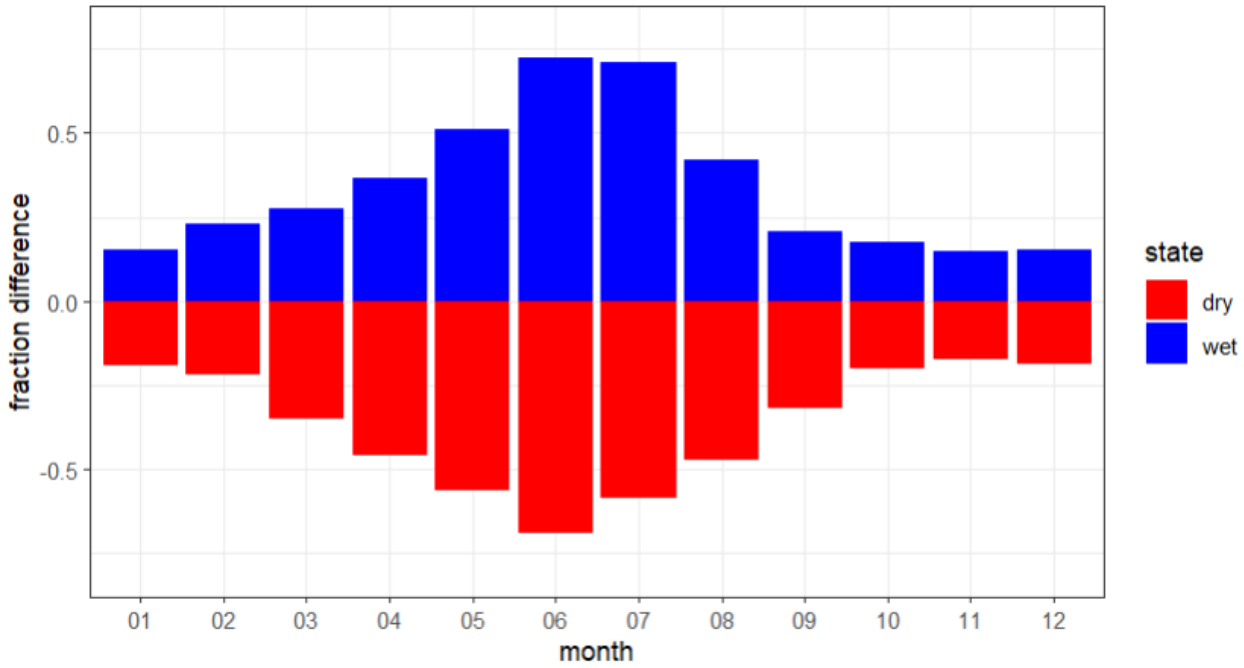

Figure 17. Median fraction difference in monthly flow (mm) between the wettest 25% and driest 25% of years compared to the mean flow over all years.

The timing of flow shifted earlier in the year for the driest years and later in the year for the wettest years compared to the timing for all years combined (Figure 18). Dry years tend to have more of the annual total flow in the winter and early spring and less during snowmelt runoff, and the reverse is true for wet years. The dates of quantiles of water year total flow can be used to estimate the timing of flow at a given location (Figure 19). The start of the hydrograph rise is at approximately 20%, and peak flow is at 60-70%.

While the model predicts quantile dates as day of water year (where day 1 is Oct 1), these can be converted to calendar year dates using the following formulas:

If day_of_water_year <= 92, day_of_calendar_year = day_of_water_year + 273 (non leap years; 274 for leap year)

If day_of_water_year > 92, day_of_calendar_year = day_of_water_year - 92

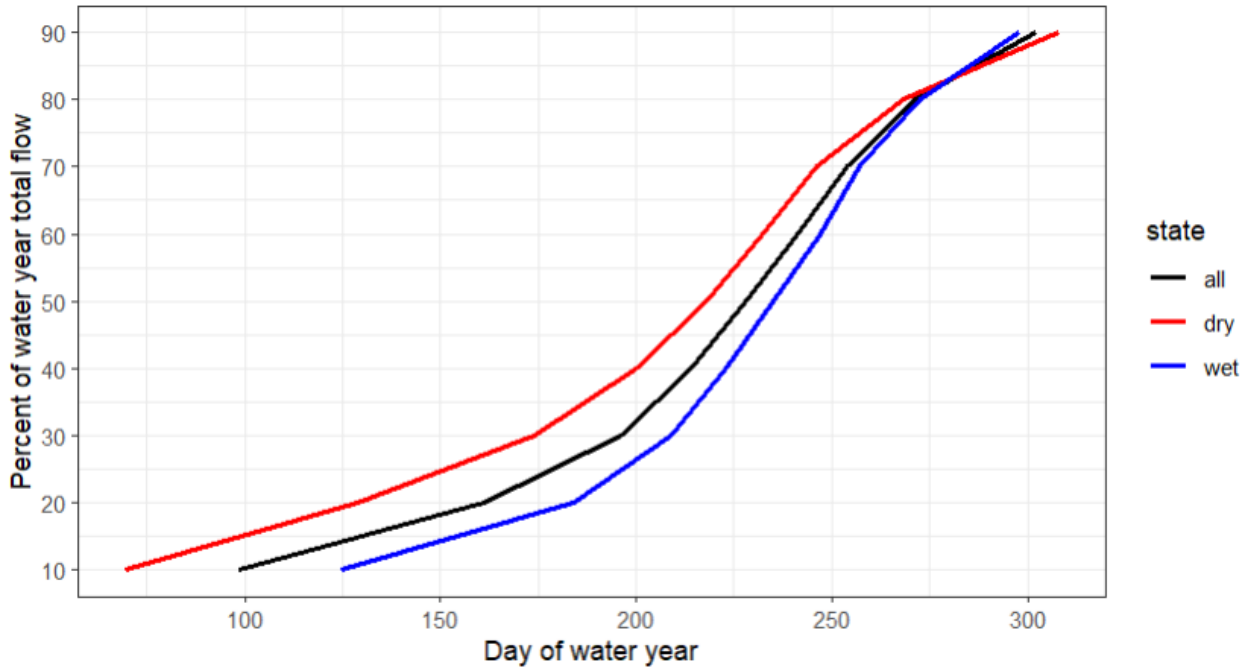

Figure 18. Percent of water year total flow vs. median day of water year for all years, the wettest 25% of years, and the driest 25% of years.

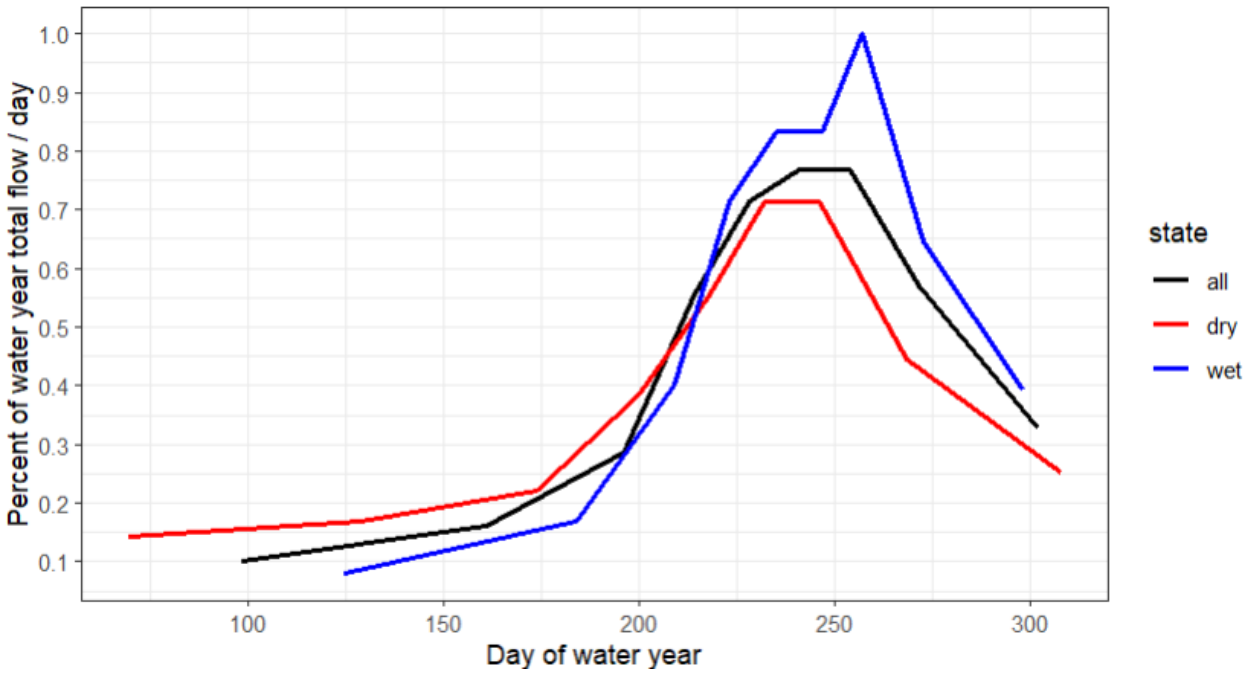

Figure 19. Derivative of Figure 7 to show the shape of the hydrograph across the water year.

3.3. Application of CSUFlow25 models

The CSUFlow25 models are integrated into an R shiny app available online at https://geocentroid.shinyapps.io/CSUFlow25/. The user can zoom to a location of interest and click on a streamline to delineate a watershed. The app will then compile the predictor variables and compute the model-predicted flow values for the watershed. The resulting predictions can then be downloaded. Values for streamflow are available in both mm and cfs, and flow quantiles are given as both day of water year and calendar state. For each variable the 95% confidence interval is provided to indicate the range of uncertainty in the prediction.

4. Discussion and conclusions

CSUFlow25 models provide predictions of mean annual and mean monthly flows, high and low flows, flow timing, monsoon flows, and bankfull flow. These models were developed using an extensively vetted dataset of streamflow from Colorado and surrounding states. Rather than using as many stations as possible to develop the models, we emphasized finding stations most likely to give accurate representations of natural streamflow. Despite this, we did include watersheds that have flow modifications contained within the watershed boundaries, as we otherwise would not have had an adequate sample size. These within-watershed flow modifications may have affected magnitudes of flow at a monthly time scale, low flows, and the timing of flow quantiles. Diversions for irrigation into a storage reservoir, for example, may reduce snowmelt runoff flows during the spring and early summer and then increase late summer and fall flows due to irrigation return flows.

Generally, the CSUFlow25 models perform better for predicting snowmelt runoff (months May-October, Qmax, Q95) than for baseflow and low flows (months November-March, Qmin, Q5). Statistical models often struggle to predict low flows, likely because these low flows are strongly affected by watershed characteristics that are not well represented by the predictor variables. These characteristics may be geological layers not captured by the simplified dominant geology (rock type) variable, soil properties not captured in the coarse soil survey data, or channel geomorphic features that dictate how much flow is released during baseflow. Although we screened out seasonally operated stream gages from the low flow month model development, it is possible that some of the sites remaining in the dataset had issues with winter ice that affected the low flow measurements. The challenges in modeling low flows also affected predictions of the fraction of flow during the monsoon season.

For flow timing, we considered several options for variables such as the start of snowmelt runoff and start of baseflow. Quantitatively identifying these start times proved to be challenging because of flow variability between sites and years. For example, snowmelt may start with a gradual rise for a few days, then stop and start again, making it unclear which start time is most representative. Similarly, for baseflow, streams usually exhibit a gradual decline in flow, which may eventually reach a steady state, though more often the flow never reaches steady state. Rain events or within-watershed flow modifications cause the flow to fluctuate during the hydrograph recession, and again it becomes unclear how best to define the onset of baseflow. For this reason we instead simulated the timing of flow quantiles, as these have an unambiguous definition and can be easily quantified for any site. Users of CSUFlow25 can use these quantiles however they choose to characterize flow timing. For a snowmelt-

dominated hydrograph, the 10-20% quantiles are likely to represent baseflow, 30-50% quantiles the hydrograph rise, 60-70% the hydrograph peak, and 80-90% the hydrograph recession (Figure 19).

Colorado has considerable flow variability between years, and if CSUFlow25 users are interested in how much the flow may differ from mean annual conditions, the values in Figure 17 provide an estimate. The differences are aligned with the snowmelt hydrograph, with flows in June about 70% higher or lower than the mean annual June flow during the wettest and driest 25% of years. The flow differences decline to a minimum of about 15% during November, December, and January. Even though the low flow month predictions are likely to be least accurate due to worse model performance, the low flows have limited variability between wet and dry years. Models for the high flow months are much stronger and more likely to be accurate for mean annual values, but high flows exhibit much more flow variability between years. This indicates that there is a tradeoff between model accuracy and interannual flow variability.

The CSUFlow25 models have some variability in performance between hydrologic regions, but generally all regions have comparable performance except the plains. This is most likely due to the small sample size of watersheds in the plains (9), which is not enough to adequately characterize the flow in a statistical model. Flow rates in the plains are also very low compared to other regions, and again the low flows are the hardest to predict.

Overall, CSUFlow25 models are an improvement over CSUFlow18 predictions and also perform better than USGS StreamStats models. Likely the main reason for these improvements was the increase in potential predictor variables, but other contributors to improved model performance may have been our expansion of the potential training sites into neighboring states and our more rigorous screening of gaging sites for transbasin diversions and other modifications. The models have very good performance for mean annual flow, June-October mean monthly flows, high flows (Qmax, Q95), and bankfull flow. May, November, low flows (Qmin, Q5), monsoon flow, and most flow quantile models during the hydrograph rise are good to satisfactory. The models for winter months (December-March) and quantiles during those time periods do not perform as well, but because these months have low flow, prediction errors are small in terms of total flow volume. Confidence intervals provided with CSUFlow25 predictions can be used to assess the likely accuracy of the modeled values.

References

Abatzoglou, J. T. (2013). Development of gridded surface meteorological data for ecological applications and modelling. International Journal of Climatology, 33, 121–131. https://doi.org/10.1002/joc.3413

Andrews, E. D. (1984). Bed-material entrainment and hydraulic geometry of gravel-bed rivers in Colorado. Geological Society of America Bulletin, 95(3), 371-378.

Capesius, J. P., & Stephens, V. C. (2009). Regional regression equations for estimation of natural streamflow statistics in Colorado, Scientific Investigations Report 2009-5136. http://pubs.usgs.gov/sir/2009/5136/

Daly, C. (2013). Descriptions of PRISM spatial climate datasets for the conterminous United States (PRISM Doc., 14 p.). Corvallis, OR: PRISM Climate Group, Oregon State University.

Daymet: Daily Surface Weather Data on a 1-km Grid for North America, Version 4 R1 https://doi.org/10.3334/ORNLDAAC/2129

Dewitz, J., 2021, National Land Cover Database (NLCD) 2019 Land Cover Science Product (ver. 2.0, June 2021): U.S. Geological Survey data release, https://doi.org/10.5066/P9KZCM54.

Eurich, A., Kampf, S. K., Hammond, J. C., Ross, M., Willi, K., Vorster, A. G., & Pulver, B. (2021). Predicting mean annual and mean monthly streamflow in Colorado ungauged basins. *River Research and Applications*, *37*(4), 569-578.

Gesch, D.B., Evans, G.A., Oimoen, M.J., Arundel, S. (2018) The National Elevation Dataset. USGS Publications Warehouse, https://pubs.usgs.gov/publication/70201572.

Hammond, J. C., Saavedra, F. A., & Kampf, S. K. (2017). MODIS MOD10A2 derived snow persistence and no data index for the western U.S. HydroShare. https://doi.org/10.4211/hs.1c62269aa802467688d25540caf2467e

Hammond, J. C., Saavedra, F. A., & Kampf, S. K. (2018). How does snow persistence relate to annual streamflow in mountain watersheds of the western US with wet maritime and dry continental climates?. *Water Resources Research*, *54*(4), 2605-2623.

Hammond, J.C., 2020, Contiguous U.S. annual snow persistence and trends from 2001-2020: U.S. Geological Survey data release, https://doi.org/10.5066/P9U7U5FP.

Hill, R.A., Weber, M.H., Leibowitz, S.G., Olsen, A.R., Thornbrugh, D.J. (2016). The Stream-Catchment (StreamCat) Dataset: A Database of Watershed Metrics for the Conterminous United States. Journal of the American Water Resources Association (JAWRA) 52:120-128. DOI: 10.1111/1752-1688.12372.

Horton, J.D., San Juan, C.A., and Stoeser, D.B. (2017). The State Geologic Map Compilation (SGMC) geodatabase of the conterminous United States (ver. 1.1, August 2017): U.S. Geological Survey Data Series 1052, 46 p., https://doi.org/10.3133/ds1052.

Moriasi, D. N., Arnold, J. G., Van Liew, M. W., Bingner, R. L., Harmel, R. D., & Veith, T. L. (2007). Model evaluation guidelines for systematic quantification of accuracy in watershed simulations. Transactions of the ASABE, 50(3), 885–900. https://doi.org/10.13031/2013.23153

Segura, C., & Pitlick, J. (2010). Scaling frequency of channel-forming flows in snowmelt-dominated streams. Water Resources Research, 46(6).

Simon, A., Dickerson, W., & Heins, A. (2004). Suspended-sediment transport rates at the 1.5-year recurrence interval for ecoregions of the United States: Transport conditions at the bankfull and effective discharge?. Geomorphology, 58(1-4), 243-262.

Vlah, M. J., Ross, M. R. V., Rhea, S., and Bernhardt, E. S.: Leveraging gauge networks and strategic discharge measurements to aid the development of continuous streamflow records, Hydrol. Earth Syst. Sci., 28, 545–573, https://doi.org/10.5194/hess-28-545-2024, 2024.

U.S. Census Bureau. (2024). *TIGER/Line shapefiles: Roads* [Data set]. U.S. Department of Commerce. https://www.census.gov/geographies/mapping-files/time-series/geo/tiger-line-file.html

Whiting, P. J., Stamm, J. F., Moog, D. B., & Orndorff, R. L. (1999). Sediment-transporting flows in headwater streams. Geological Society of America Bulletin, 111(3), 450-466.

Appendix A1. Dataset documentation

Table A1. Included sites: Sites that passed all filters and are used in model development and testing. Natural sites have no flow modifications that we identified; modified have some type of flow modification mentioned in the USGS remarks or evident in the dam and urban metrics obtained for the watersheds. Sites in grey are seasonally operated and were used only for the months for which the data completeness criteria were met.

USGS ID	CDWR ID	Name	Class
06309200		Middle Fork Powder River Near Barnum, WY	natural
06622700		North Brush Creek Near Saratoga, WY	natural
06632400		Rock Creek AB King Canyon Canal, NR Arlington, WY	modified
06755960		Crow Creek at 19th Street, at Cheyenne, WY	modified
06823500		Buffalo Creek near Haigler, NB	modified
06824000		Rock Creek at Parks, NB	modified
06836500		Driftwood Creek near McCook, NB	modified
07203000		Vermejo River Near Dawson, NM	modified
07207500		Ponil Creek Near Cimarron, NM	modified
07208500		Rayado Creek Near Cimarron, NM	natural
07218000		Coyote Creek Near Golondrinas, NM	modified
08267500		Rio Hondo Near Valdez, NM	natural
08269000		Rio Pueblo de Taos Near Taos, NM	natural
08271000		Rio Lucero Near Arroyo Seco, NM	natural
08275500		Rio Grande del Rancho Near Talpa, NM	modified
08277470		Rio Pueblo NR Penasco, NM	natural
08289000		Rio Ojo Caliente at La Madera, NM	modified
08291000		Santa Cruz River Near Cundiyo, NM	modified
08302500		Tesuque Creek Above Diversions Near Santa Fe, NM	natural
08315480		Santa Fe River Above Mcclure Res, NR Santa Fe, NM	natural
08324000		Jemez River Near Jemez, NM	modified

USGS ID	CDWR ID	Name	Class
08334000		Rio Puerco Abv Arroyo Chico NR Guadalupe, NM	natural
08377900		Rio Mora Near Terrero, NM	natural
08380500		Gallinas Creek Near Montezuma, NM	natural
09025300		Elk Creek at Upper Station, Near Fraser, CO	natural
09066000		Black Gore Creek Near Minturn, CO	modified
09066300		Middle Creek Near Minturn, CO	modified
09217900		Blacks Fork Near Robertson, WY	natural
09220000		East Fork of Smiths Fork Near Robertson, WY	modified
09279000		Rock Creek Near Mountain Home, UT	modified
09289500		Lake Fork River AB Moon Lake, NR Mountain Home, UT	natural
09292000		Yellowstone R @ Bridge Cmpgrnd Nr Altonah, UT	modified
09296800		Uinta R Blw Powerplant Diversion, NR Neola, UT	modified
09299500		Whiterocks River Near Whiterocks, UT	modified
09378170		South Creek Above Reservoir Near Monticello, UT	natural
09378630		Recapture Creek Near Blanding, UT	natural
09386900		Rio Nutria Near Ramah, NM	natural
401733105392404		The Loch Outlet	natural
07105000	BEARCOCO	Bear Creek Near Colorado Springs, CO	modified
06725500	BOCMIDCO	Middle Boulder Creek at Nederland, CO	natural
402114105350101	BTBMORCO	Big Thompson BL Moraine Park NR Estes Park, CO	natural
07103703	CAMPGOCO	Camp Creek at Garden of the Gods, CO	modified
07122400	CANSWKCO	Crooked Arroyo Near Swink, CO	modified
09358550	CEMSILCO	Cement Creek at Silverton, CO	modified
07091015	CHCRNACO	Chalk Creek at Nathrop	natural
07105490	CHEEVACO	Cheyenne Creek at Evans Ave at Colorado Springs, CO	modified
06712000	CHENEFCO	Cherry Creek Near Franktown, CO	modified

USGS ID	CDWR ID	Name	Class
	CHEREDCO	Cherry Creek at the Mouth Near Red Mesa	natural
07089250	COCRBVCO	Cottonwood Creek Near Buena Vista	natural
07114000	CRBRLVCO	Cucharas River at Boyd Ranch, Near La Veta, CO	modified
	CRHBLVCO	Cucharas River at Harrison Bridge Near La Veta, CO	natural
09065100	CROMINCO	Crow Creek Near Minturn, CO	modified
09081600	CRYAVACO	Crystal River Abv Avalanche Crk, Near Redstone, CO	modified
	ERIRGRCO	East Rifle Creek Above Rifle Gap Reservoir	modified
09238900	FISCRECO	Fish Cr at Upper Sta Nr Steamboat Springs, CO	modified
09362750	FLOALECO	Florida River Above Lemon Reservoir NR Durango, CO	modified
07095000	GRAWESCO	Grape Creek Near Westcliffe, CO	natural
07083000	HALMALCO	Halfmoon Creek Near Malta, CO	modified
	HAYREDCO	Hay Gulch Above Red Mesa Rservoir	natural
07111000	HURREDCO	Huerfano R at Manzanares Xing, NR Redwing, CO	modified
07105900	JIMCAMCO	Jimmy Camp Creek at Fountain, CO	modified
08224500	KERVILCO	Kerber CR Abv Little Kerber CR NR Villa Grove, CO	modified
09047700	KEYGUDCO	Keystone Gulch Near Dillon, CO	natural
08231000	LAGLAGCO	La Garita Creek Near La Garita, CO	natural
09124500	LAKFORCO	Lake Fork at Gateview, CO	modified
08248000	LOSORTCO	Los Pinos River Near Ortiz, CO	modified
09253000	LSRSLACO	Little Snake River Near Slater, CO	modified
07126100	LUARMOCO	Luning Arroyo Near Model, CO	natural
	MANMANCO	Mancos River Near Mancos	natural
09344000	NAVBANCO	Navajo R at Banded Peak Ranch, Near Chromo, CO	modified
09306200	PICRYACO	Piceance Creek BL Ryan Gulch, NR Rio Blanco, CO	modified
09059500	PINSTBCO	Piney River Near State Bridge, CO	modified
06708800	PLUCASCO	East Plum Cr Abv Haskins Gulch Nr Castle Rock, CO	modified
07124200	PURMADCO	Purgatoire River at Madrid, CO	modified

USGS ID	CDWR ID	Name	Class
	RALCRKCO	Ralston Creek Above Ralston Reservoir Near Golden	natural
	SANCRECO	San Isabel Creek Near Crestone	natural
08241500	SANFTGCO	Sangre de Cristo Creek Near Fort Garland, CO	modified
08247500	SANORTCO	San Antonio River at Ortiz, CO	modified
09255000	SLAFORCO	Slater Fork Near Slater, CO	modified
09077000	SNOCRECO	Snowmass Creek	modified
09107000	TAYATPCO	Taylor River at Taylor Park, CO	natural
07121500	TIMSWICO	Timpas Creek at Mouth Near Swink, CO	modified
08240500	TRITURCO	Trinchera Creek Above Turner's Ranch	natural
09352900	VALBAYCO	Vallecito Creek Near Bayfield, CO	natural
	WESRIFCO	West Rifle Creek Above Rifle Gap Reservoir	modified
09306255	YELWHICO	Yellow Creek Near White River, CO	modified
08220500	PINDELCO	Pinos Creek Near Del Norte, CO	modified
06739500	BUCRMVCO	Buckhorn Creek Near Masonville, CO	natural
08230500	CARLAGCO	Carnero Creek Near La Garita, CO	modified
	CHECRECO	Wild Cherry Creek Near Crestone	natural
06730300	COCREPCO	Coal Creek Near Plainview, CO	natural
08229500	COCRESCO	Cottonwood Creek Near Crestone, CO	natural
08226700	COCRMICO	Cotton Creek Near Mineral Hot Springs, CO	modified
	GARVILCO	Garner Creek Near Villa Grove	natural
	MAJVILCO	Major Creek Near Villa Grove	modified
	RITCRECO	Rito Alto Creek Near Crestone	natural
	SOUCRECO	Soth Crestone Creek Near Crestone	natural
	SPACRECO	Spanish Creek Near Crestone	natural
	WILCRECO	Willow Creek Near Crestone	natural
09112200	EASCEMCO	East River Below Cement Creek Nr Crested Butte, CO	modified
09246200	ELKLONCO	Elkhead Creek Above Long Gulch, Near Hayden, CO	modified

USGS ID	CDWR ID	Name	Class
	MEDSANCO	Medano Creek at Great Sand Dunes National Park	natural
09041090	MUDAACCO	Muddy Creek Above Antelope Creek Nr. Kremmling, CO	modified
07126200	VANMODCO	Van Bremer Arroyo Near Model, CO	modified
07134990	WILDHOCO	Wild Horse Creek Above Holly, CO	modified
08235270	WFKCROCO	Wightman Fork Below Cropsey Creek at Summitville	modified
	LKCTURCO	Lake Fork Creek Above Turquoise	natural
08227500	NOCRESCO	North Crestone Creek Near Crestone, CO	natural
06722500	SSVWARCO	South Saint Vrain Near Ward	natural
	MIDSTECO	Middle Saint Vrain at Peaceful Valley	natural
08238000	LAJCAPCO	La Jara Creek at Gallegos Ranch, NR Capulin, CO	modified
06724000	SVCLYOCO	Saint Vrain Creek at Lyons, CO	modified
08242500	UTEFTGCO	Ute Creek Near Fort Garland, CO	modified
07099060	BEAPENCO	Beaver Creek above Highway 115, Near Penrose, CO	modified
	TROGARCO	Trout Creek Near Garo	natural
	FOUHIGCO	Four Mile at High Creek	natural
	RCKTARCO	Rock Creek Above Confluence with Tarryall Creek	natural
09242500	ELKMILCO	Elk River Near Milner, CO	modified
	FRYNFNCO	North Fork Fryingpan River Near Norrie, CO	natural
07086500	CCACCRCO	Clear Creek Above Clear Creek Reservoir, CO	natural
09165000	DOLRICCO	Dolores River Below Rico, CO	natural
07084500	LAKATLCO	Lake Creek Above Twin Lakes Reservoir, CO	natural
	MFKABMCO	Middle Fork South Platte Above Montgomery Rservoir Near Alma	natural
	SANDUNCO	Sand Creek at Great Sand Dunes National Park	natural
	WINDESCO	Wind River Near Estes Park	natural
08253000	CASCOSNM	Casias Creek Near Costilla, NM	modified
06698000	JEFJEFCO	Jefferson Creek Near Jefferson	modified

USGS ID	CDWR ID	Name	Class
	LTCANYCO	Little Thompson River at Canyon Mouth Near Berthod	natural
	OHGJEFCO	Ohler Gulch Near Jefferson	natural
	SFKANTCO	South Fork of South Platte Above Antero	natural
08218500	GOOWAGCO	Goose Creek at Wagonwheel Gap, CO	modified

Columns in the dataset:

Identifying information

- cdwr_id: ID code for gages from the Colorado Division of Water Resources
- usgs_id: site number for gages from USGS
- name: name of stream gage
- usable: indicates whether all months passed the data completeness filter. “all” indicates all months passed the filter. Otherwise the column lists the months that passed the filter.

Data quality information

- min_date: first date with data starting in WY2000
- max_date: last date with data up to end of WY2024
- missing_days: count of days with missing data
- percent_missing: percent of days with missing data. Percent missing also provided for each month.
- estimates: USGS flags flow values that are estimated. This is a count of days with the estimate flag. These values are not included for CDWR sites.

Streamflow variables

- Qann: mean annual streamflow total (mm)
- Qjan-Qdec: mean monthly streamflow total (mm)
- Qmax: mean annual maximum daily streamflow (mm/d)
- Qmin: mean annual minimum daily streamflow (mm/d)
- Q95: 95th percentile flow from flow duration curve (mm/d)
- Q5: 5th percentile flow from flow duration curve (mm/d)
- Day10-Day90: day of water year when 10% to 90% (in increments of 10%) of water year total flow has passed the stream gage
- monsoon: mean annual fraction of water year total flow that comes in July, August, and September
- bankfull: 1.5 year return period flow (mm/d)

Predictor variables

- area: drainage area of watershed in km2
- elevation: mean elevation of watershed in m

- area60: fraction of watershed with mean annual snow persistence >60%
- slope: mean slope of watershed (fraction)
- slope30: fraction of watershed with slopes >30% (0.3)
- aspect: aspect direction that covers the largest area in the watershed
- northness: mean northness of all grid cells in the watershed
- north_fraction: fraction of grid cells with N, NE, NW aspects
- Pann: mean annual total precipitation (mm)
- Ppeak: maximum monthly precipitation (mm)
- Pjan-Pdec: mean monthly total precipitation (mm)
- SWEjan-SWEjun: mean monthly snow water equivalent (mm)
- SWEpeak: average annual peak snow water equivalent (mm)
- SP: mean annual (2001-2020) January 1 - July 3 snow persistence (%)
- PET: mean annual grass reference evapotranspiration (mm)
- geology: bedrock geology type covering the largest area in the watershed (categorical)
- region: hydrologic region (categorical)
- forest: percent of watershed area that is forested
- grassland: percent of watershed area that is grassland / herbaceous
- shrub: percent of watershed area that is shrubland
- agriculture: percent of watershed area that is agriculture
- impervious: percent of watershed area that is impervious
- road: road density as road length per drainage area (km/km2)
- sand: percent of sand in soil, averaged over watershed area
- clay: percent of clay in soil, averaged over watershed area
- bedrock: average depth to bedrock in watershed (mm)
- watertable: average depth to water table in watershed (mm)
- permeability: average permeability of soils in watershed (cm/hr)

Table A2. Excluded sites: Sites excluded from the model development dataset and the reason for exclusion. Many sites have more than one reason for exclusion, but only the first reason for exclusion is listed here. Reasons could be a dam at the watershed outlet that might have a large influence on flow, did not meet data criteria, has transbasin diversions, or did not meet urban criteria. Sites labeled downstream are downstream of another gage or gages included in the dataset; these were removed to avoid double-counting flow metrics. One gage is excluded because it has a mixture of modifications; none met the exclusion criteria directly, but the large number of modifications together made us conclude that this gage was not suitable for modeling.

USGS ID	CDWR ID	Reason for exclusion
07206000		dam
08213500	RIOMILCO	dam
08214500	NCLCONCO	dam
08294210		dam
	BEVBEVCO	dam
	DOUOUTCO	dam
	WILBSLCO	dam
08254000	COSBELNM	dam
08245000	CONPLACO	dam
07099050	BEACEMCO	data limited
	BIGSPGCO	data limited
09099550	BIGUPPCO	data limited
09066200	BOOMINCO	data limited
06736000	BTNFDRCO	data limited
09077945	CHAGULCO	data limited
	CHIDEVCO	data limited
	CLEGLKCO	data limited
09306242	CORNRACO	data limited
06727500	FOUOROCO	data limited
	FRNCRKCO	data limited
09077200	FRYIVLCO	data limited

USGS ID	CDWR ID	Reason for exclusion
09077800	FRYSFUCO	data limited
09065500	GORUPPCO	data limited
07112500	HUEBADCO	data limited
06724500	LEFCRECO	data limited
	LONREDCO	data limited
06614800	MIRICACO	data limited
09113500	OHIBALCO	data limited
09093500	PARPARCO	data limited
08284100	RCHLAPNM	data limited
08253500	SANCOSNM	data limited
06696980	TARUPPCO	data limited
09040500	TROUBLCO	data limited
06718550	NCCBLACO	data limited
	CULCHACO	data limited
	ELKNEWCO	data limited
07105945	ROCAFOCO	data limited
08220900	SAFUPPCO	data limited
09363100	SALTOXCO	data limited
07099230	TURTELCO	data limited
06715000		downstream
08250000		downstream
09078500	FRYTHOCO	downstream
09359020	ANIBSICO	downstream
09050700	BLUDILCO	downstream
09057500	BLUGRECO	downstream
	CCBCCRCO	downstream
06719505	CLEGOLCO	downstream

USGS ID	CDWR ID	Reason for exclusion
06715000	CLEWFOCO	downstream
08250000	COSCOSNM	downstream
09067020	EAGAVOCO	downstream
09080400	FRYRUDCO	downstream
09066510	GORCRECO	downstream
09066325	GORREDCO	downstream
	LITSPGCO	downstream
09354500	LOSLABCO	downstream
09041400	MUDKRECO	downstream
09132500	NFGSOMCO	downstream
09113980	OHIOCRCO	downstream
06709000	PLUSEDCO	downstream
	RIOMOUCO	downstream
09110000	TAYALMCO	downstream
09109000	TAYBERCO	downstream
09147025	UNCBRRCO	downstream
09147500	UNCCOLCO	downstream
09035700	WILDARCO	downstream
09038500	WILFORCO	downstream
09036000	WILLEACO	downstream
09037500	WILPARCO	downstream
09239500	YAMSTECO	downstream
06625000		downstream
08276300		downstream
08279000		downstream
08316000		downstream
08378500		downstream

USGS ID	CDWR ID	Reason for exclusion
09291000		downstream
09292500		downstream
09409100		downstream
10130500		downstream
08236500	ALABELCO	downstream
08235250	ALAWIGCO	downstream
09359500	ANITIMCO	downstream
07087050	ARKBGNCO	downstream
07083710	ARKEMPCO	downstream
07086000	ARKGRNCO	downstream
07081200	ARKLEACO	downstream
06710605	BCRABCCO	downstream
06710500	BCRMORCO	downstream
	BCROUTCO	downstream
06711500	BCRSHECO	downstream
07099060	BEAPENCO	downstream
06730500	BOCLONCO	downstream
06727000	BOCOROCO	downstream
06733000	BTABESCO	downstream
06713000	CHEBELCO	downstream
06713500	CHEDENCO	downstream
393109104464500	CHERRYCO	downstream
09127000	CIMSQWCO	downstream
06720000	CLEDERCO	downstream
06716500	CLELAWCO	downstream
07103990	COCRPICO	downstream
09019500	COLNGBCO	downstream

USGS ID	CDWR ID	Reason for exclusion
	CONCONCO	downstream
08254000	COSBELNM	downstream
08261000	COSGARCO	downstream
	DIXCOMCO	downstream
09166500	DOLDOLCO	downstream
09112500	EASALMCO	downstream
09246500	ELKCRACO	downstream
	FLOBLECO	downstream
09363200	FLOBONCO	downstream
09363050	FLOFARCO	downstream
07105500	FOUACSCO	downstream
	FOUHARCO	downstream
07105530	FOUJANCO	downstream
07105800	FOUSECCO	downstream
09033300	FRATABCO	downstream
09080100	FRYMERCO	downstream
09064000	HOMGOLCO	downstream
	JEFSNYCO	downstream
	LAKBTLCO	downstream
07082500	LFCBSLCO	downstream
06697450	MCHJEFCO	downstream
	MEROUTCO	downstream
	MFKBLMCO	downstream
07104000	MONPIKCO	downstream
07103970	MONWOOCO	downstream
	MTNOUTCO	downstream
	NAVOSOCO	downstream

USGS ID	CDWR ID	Reason for exclusion
	NORCONCO	downstream
	PLAANTCO	downstream
	PLABAICO	downstream
06709530	PLUTIRCO	downstream
09080300	RANMEACO	downstream
	RIFRGRCO	downstream
	ROABMCCO	downstream
08248500	SANMANCO	downstream
	SUGARCCO	downstream
06725450	SVCBLOCO	downstream
	TARBORCO	downstream
	TARTARCO	downstream
08241000	TRIMTNCO	downstream
08243500	TRISMICO	downstream
08235290	WFKMOUCO	downstream
	YAMBELCO	downstream
07207000		downstream
09271000		downstream
10016900		downstream
07103780	MONGATCO	multiple modifications
	BOBCRKCO	transbasin
	LINGRRCO	transbasin
	LVNGEOCO	transbasin
	MERINFCO	transbasin
	MUDHIGCO	transbasin
	SMILAZCO	transbasin
08227000	SAGSAGCO	transbasin

USGS ID	CDWR ID	Reason for exclusion
06711040	TURBCRCO	transbasin
	KANJUNCO	transbasin
09365500	LAPHESCO	transbasin
09343300	RIOBLACO	transbasin
	LITOSOCO	transbasin
09085500	CANNEWCO	transbasin
09035900		transbasin
09063900		transbasin
08236000	ALATERCO	transbasin
09358000	ANISILCO	transbasin
07079300	ARKEFOCO	transbasin
06710385	BCREVRCO	transbasin
09067000	BEAVONCO	transbasin
06741510	BIGLOVCO	transbasin
09046490	BLUABLCO	transbasin
09034900	BOBJOPCO	transbasin
09032100	CABFRACO	transbasin
09118450	CHETOPCO	transbasin
09126000	CIMCIMCO	transbasin
06751490	CLANLICO	transbasin
09010500	COLBAKCO	transbasin
08246500	CONMOGCO	transbasin
09064600	EAGMINCO	transbasin
07103700	FOUNCOCO	transbasin
09024000	FRAWINCO	transbasin
06746110	JOEBELCO	transbasin
09067200	LAKNEDCO	transbasin

USGS ID	CDWR ID	Reason for exclusion
09366500	LAPMEXCO	transbasin
09166950	LOSDOLCO	transbasin
09353800	LOSIGNCO	transbasin
09371000	MANTOWCO	transbasin
09372000	MCELMSCO	transbasin
09371520	MCELMZCO	transbasin
09359010	MINASICO	transbasin
07103800	MONAIRCO	transbasin
07103797	MONRAMCO	transbasin
06751150	NOCALACO	transbasin
09032000	RANFRACO	transbasin
08219500	RIOSFKCO	transbasin
09073400	ROAASPCO	transbasin
09073300	ROADIFCO	transbasin
08227000	SAGSAGCO	transbasin
09342500	SANPAGCO	transbasin
09026500	SLOFRACO	transbasin
07108900	STCHARCO	transbasin
09051050	STRABLCO	transbasin
09143500	SURACECO	transbasin
09050100	TENFRICO	transbasin
09146200	UNCRIDCO	transbasin
09025000	VASWINCO	transbasin
06716100	WFCEMPCO	transbasin
09304500	WHIMEECO	transbasin
09021000	WILWCRCO	transbasin
09237450	YAMSTACO	transbasin

USGS ID	CDWR ID	Reason for exclusion
06623800		transbasin
07216500		transbasin
08266820		transbasin
09229500		transbasin
09266500		transbasin
09277500		transbasin
09288000		transbasin
09310500		transbasin
10105900		transbasin
10109000		transbasin
10149000		transbasin
10157500		transbasin
	BIGHILCO	transbasin
09046600	BLUNDICO	transbasin
	BLUNINCO	transbasin
06729450	BOCBGRCO	transbasin
	BOCELSCO	transbasin
	BOCPINCO	transbasin
09147000	DALRIDCO	transbasin
09063000	EAGREDCO	transbasin
09022000	FRAUPPCO	transbasin
09074000	HUNTASCO	transbasin
06617500	ILLRANCO	transbasin
09077610	IVCRNACO	transbasin
06746095	JOECRECO	transbasin
06657500	LARRIVCO	transbasin
	MFKPRICO	transbasin

USGS ID	CDWR ID	Reason for exclusion
	MFKSTMCO	transbasin
	MICMERCO	transbasin
06617100	MICWLDCO	transbasin
09131490	MUDAPRCO	transbasin
	MUDBPRCO	transbasin
	PINBVACO	transbasin
	PLAGRACO	transbasin
	SANCRKCO	transbasin
09172500	SMGPLACO	transbasin
09129600	SMILAZCO	transbasin
	SNAKEYCO	transbasin
09047500	SNAMONCO	transbasin
	SPRBRNCO	transbasin
09143000	SURCEDCO	transbasin
09115500	TOMSARCO	transbasin
06711040	TURBCRCO	transbasin
09035500	WILSTECO	transbasin
09238500	WLTNCKCO	transbasin
09089500	WSDRAVCO	transbasin
09237500	YAMBSRCO	transbasin
07215500		transbasin
09183500		transbasin
09261700		transbasin
	COSABONM	transbasin
06720460	FIRBUCCO	urban
07103980	COCRWOCO	urban
06730200	BOCNORCO	urban

USGS ID	CDWR ID	Reason for exclusion
06720330	BIGDAFCO	urban
06720820	BIGWESCO	urban
394839104570300	SANCOMCO	urban

Appendix B: Predictor variables for the CSUFlow25 models

Table B1. Predictor variables for each streamflow variable modeled in CSUFlow25

Streamflow variable	Predictor variables
Qann	slope, SWEmar, forest, grassland, road
Qjan	region, northness, north_fraction, SP, forest
Qfeb	aspect, SP, shrub, road, watertable
Qmar	region, Pdec, SP, shrub, watertable
Qapr	region, aspect, geology, Pjan, shrub, bedrock, watertable
Qmay	region, geology, Pmay, SWEfeb, forest, grassland, watertable, sand
Qjun	geology, SWEmay, slope, northness, forest, grassland, road, sand
Qjul	geology, SWEpeak, slope, northness, forest, shrub, watertable, sand
Qaug	SWEpeak, slope, northness, elevation, forest, shrub, watertable, sand
Qsep	geology, Psep, slope, area60, forest, shrub, watertable, sand
Qoct	Paug, Psep, slope, area60, forest, shrub, sand
Qnov	region, slope, area60, shrub, agriculture, road
Qdec	region, slope, north_fraction, area60, shrub
Qmax	region, SWEapr, Pmay, agriculture, sand
Q95	SWEmar, forest, grassland, road, watertable
Qmin	Pmay, area60, shrub, permeability, sand
Q5	Pjun, area60, shrub, permeability, sand
Day10	region, Pfeb, Pmay, Psep, clay
Day20	region, SWEpeak, Pmay, Psep, clay
Day30	region, SWEapr, Pjul, Psep, permeability
Day40	SWEapr, Pjul, Psep, agriculture, sand
Day50	SWEmay, Paug, Psep, agriculture, sand
Day60	SWEmay, Paug, Psep, watertable, sand
Day70	region, SWEjun, Paug, watertable, sand
Day80	region, SWEjun, Paug, watertable, sand
Day90	region, SWEjun, Paug, Ppeak, bedrock

Streamflow variable	Predictor variables
monsoon	region, SWEjun, Paug, watertable, sand
bankfull	SWEmar, Pmay, road, watertable, sand

Appendix C: Comparison of models with fixed axes

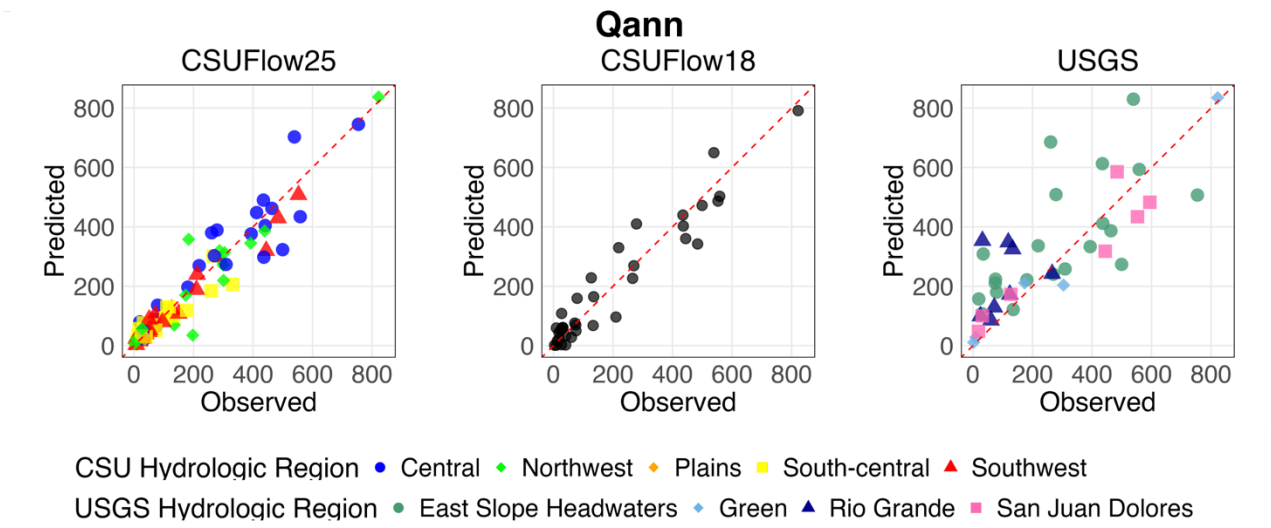

Figure C1. Predicted vs. observed mean annual total flow across the three models compared in this report, with all axes fixed.

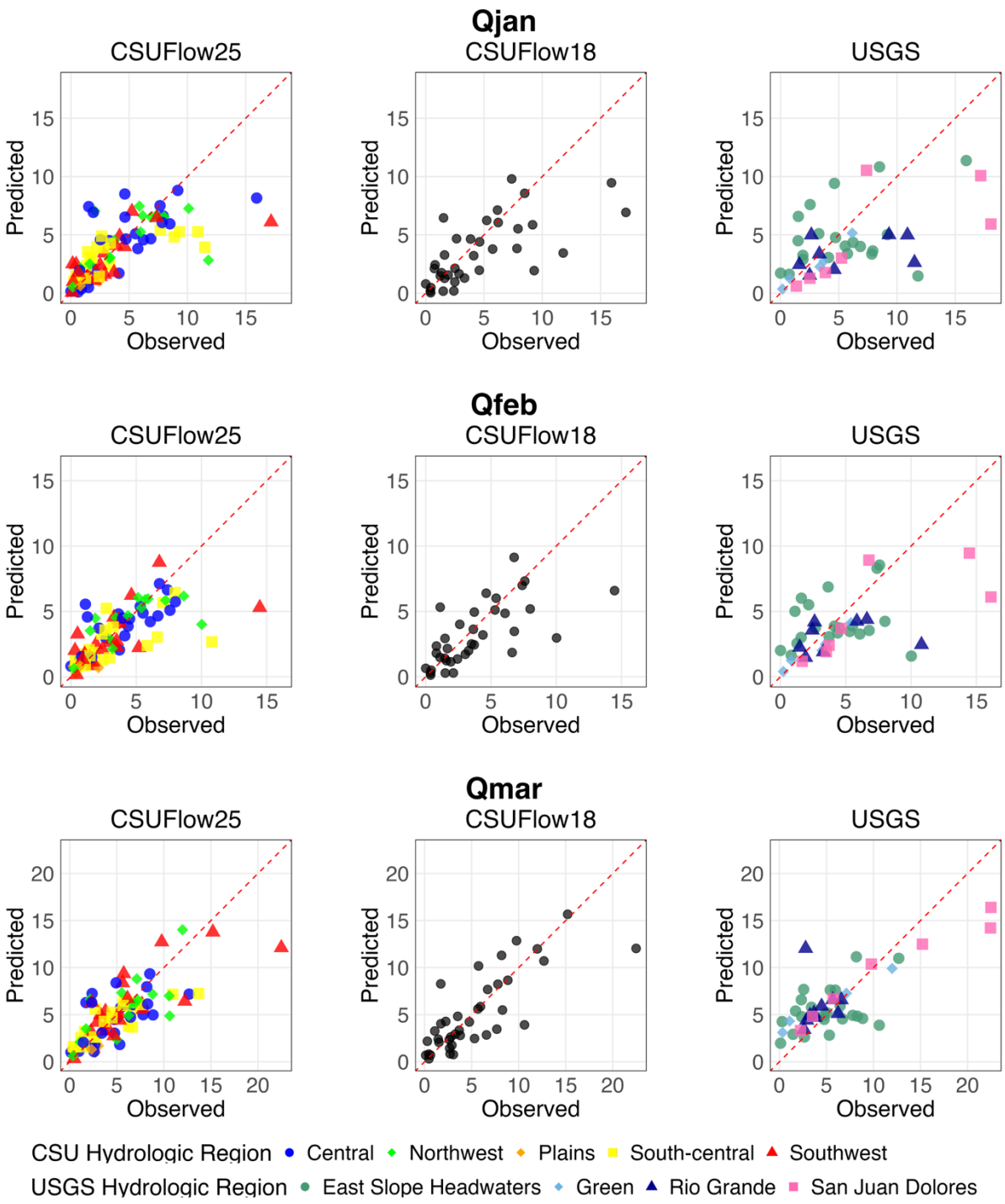

Figure C2. Predicted vs. observed mean flow in January, February, and March across the three models compared in this report, with all axes fixed.

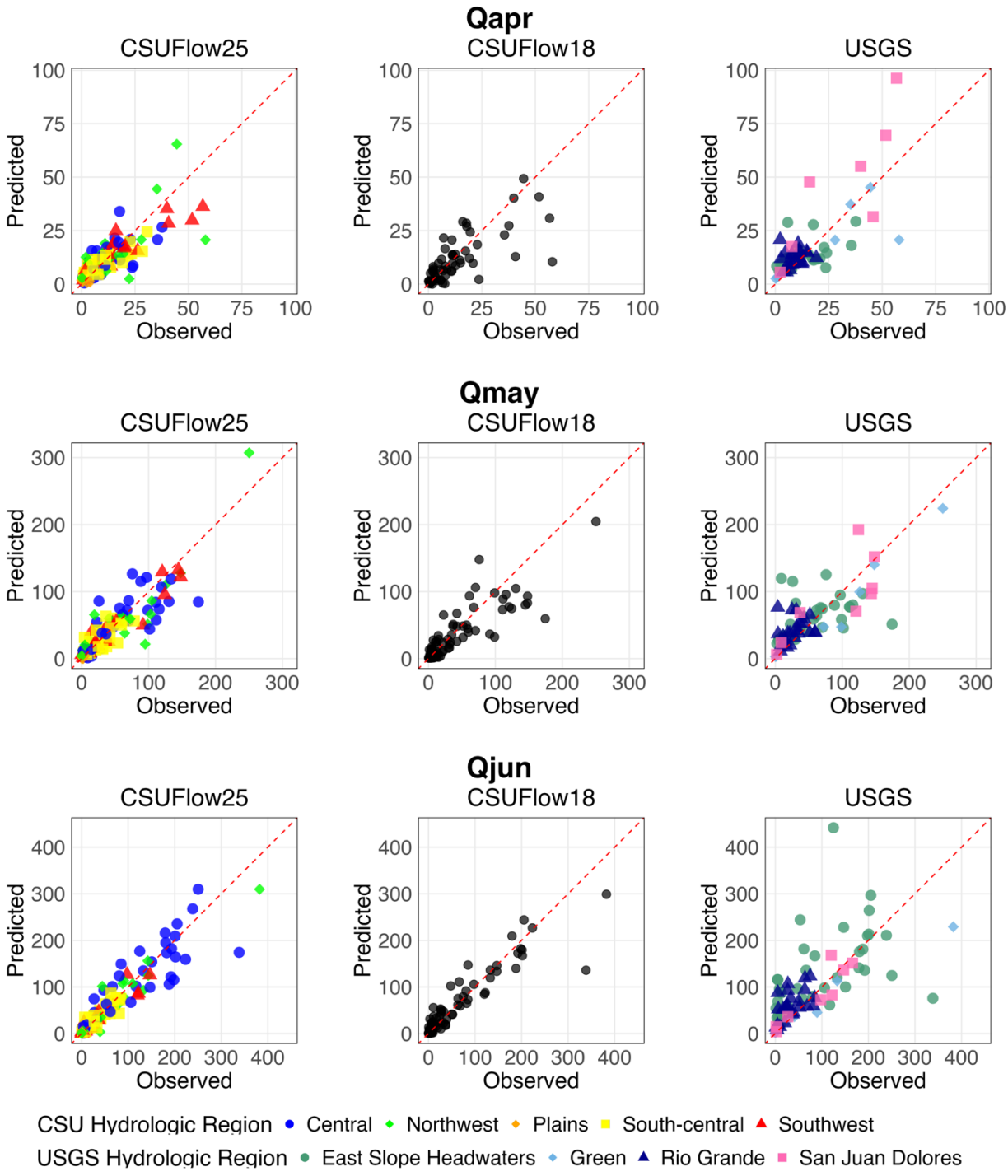

Figure C3. Predicted vs. observed mean flow in April, May, and June across the three models compared in this report, with all axes fixed.

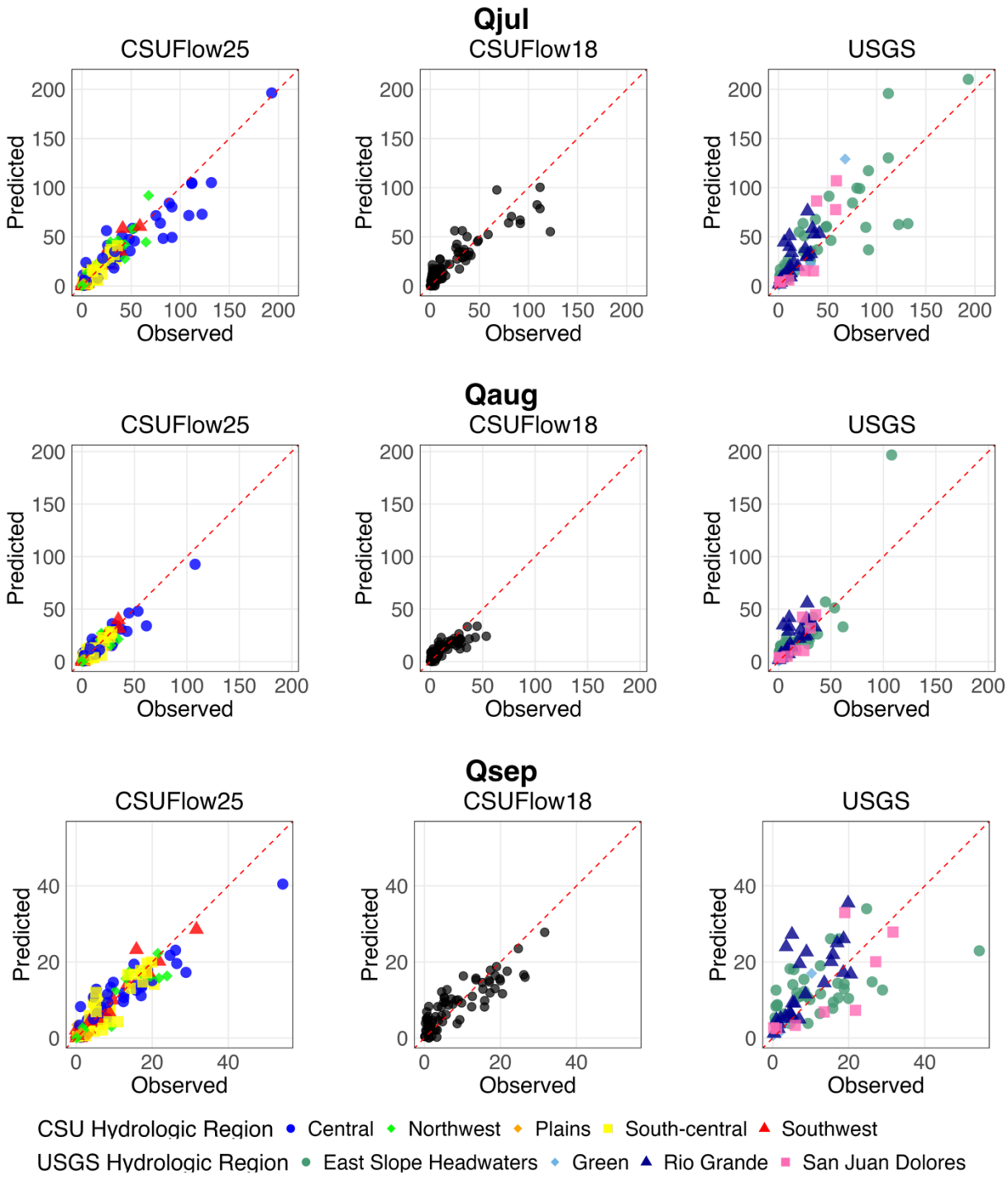

Figure C4. Predicted vs. observed mean flow in July, August, and September across the three models compared in this report, with all axes fixed.

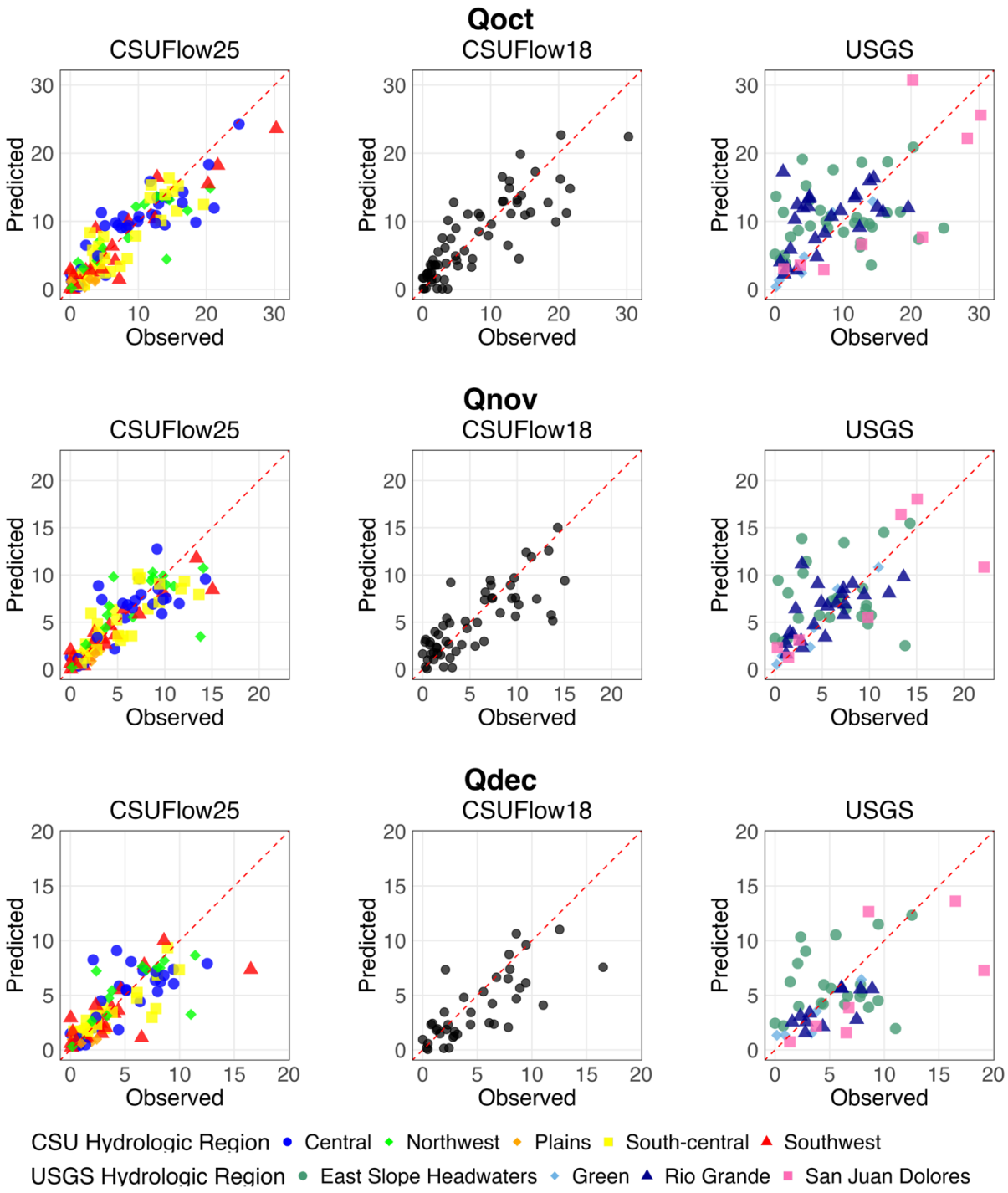

Figure C5. Predicted vs. observed mean flow in October, November, and December across the three models compared in this report, with all axes fixed.